Interacting scenarios with dynamical dark energy: observational constraints and alleviation of the H_0 tension

Supriya Pan,[1,*] Weiqiang Yang,[2,†] Eleonora Di Valentino,[3,‡]
Emmanuel N. Saridakis,[4,5,6,§] and Subenoy Chakraborty[7,¶]

[1]*Department of Mathematics, Presidency University, 86/1 College Street, Kolkata 700073, India.*
[2]*Department of Physics, Liaoning Normal University, Dalian, 116029, P. R. China.*
[3]*Jodrell Bank Center for Astrophysics, School of Physics and Astronomy, University of Manchester, Oxford Road, Manchester, M13 9PL, UK.*
[4]*Department of Physics, National Technical University of Athens, Zografou Campus GR 157 73, Athens, Greece*
[5]*Department of Astronomy, School of Physical Sciences, University of Science and Technology of China, Hefei 230026, P.R. China*
[6]*Chongqing University of Posts & Telecommunications, Chongqing, 400065, P.R. China*
[7]*Department of Mathematics, Jadavpur University, Kolkata 700032, West Bengal, India*

arXiv:1907.07540v2 [astro-ph.CO] 20 Oct 2019

We investigate interacting scenarios which belong to a wider class, since they include a dynamical dark energy component whose equation of state follows various one-parameter parametrizations. We confront them with the latest observational data from Cosmic Microwave Background (CMB), Joint light-curve (JLA) sample from Supernovae Type Ia, Baryon Acoustic Oscillations (BAO), Hubble parameter measurements from Cosmic Chronometers (CC) and a gaussian prior on the Hubble parameter H_0. In all examined scenarios we find a non-zero interaction, nevertheless the non-interacting case is allowed within 2σ. Concerning the current value of the dark energy equation of state for all combination of datasets it always lies in the phantom regime at more than two/three standard deviations. Finally, for all interacting models, independently of the combination of datasets considered, the estimated values of the present Hubble parameter H_0 are greater compared to the ΛCDM-based Planck's estimation and close to the local measurements, thus alleviating the H_0 tension.

PACS numbers: 98.80.-k, 95.36.+x, 98.80.Es

I. INTRODUCTION

After almost 20 years from the detection of late-time universe acceleration, and due to the appearance of a huge amount of data, people are still looking for the actual underlying theory that could explain it. In general, there are two widely accepted approaches that could accommodate it. The first one is the introduction of some hypothetical dark energy fluid [1] in the context of Einstein's gravitational theory. The second one is to consider modified or alternative gravitational theories where the extra geometrical terms may reproduce the effects of dark energy [2, 3, 4].

On the other hand, a mutual interaction between the dark matter and dark energy sectors was initially introduced in order to investigate the cosmological constant problem [5]. However, later on it was found that it could also alleviate the cosmic coincidence problem in a natural way [6, 7, 8, 9, 10, 11] , and this led to many investigations of interacting cosmology [12, 13, 14, 15, 16, 17, 18, 19, 20, 21, 22, 23, 24, 25, 26, 27, 28, 29, 30, 31, 32, 33, 34, 35, 36, 37, 38, 39, 40, 41, 42, 43, 44, 45, 46, 47, 48, 49, 50, 51, 52, 53, 54, 55, 56, 57, 58, 59, 60, 61] (also see [62, 63] for recent reviews on interacting dark matter-dark energy scenarios). An additional advantage of interacting scenarios is the easy realization of the phantom-divide crossing without theoretical ambiguities [64, 65, 66]. Finally, interacting scenarios prove to be efficient in alleviating the two known tensions of modern cosmology, namely the H_0 one [67, 68, 69, 70, 71, 72, 73, 74, 75, 76, 77, 78, 79, 80, 81, 82, 83, 84, 85, 86, 87, 88, 89, 90, 91, 92, 93, 94, 95], and the σ_8 one [90, 96, 97, 98].

Despite the extended investigation of interacting scenarios, the choice of the interaction function remains unknown. Thus, in general one considers phenomenological models for the interaction form and explores the cosmological dynamics confronting with observational data. The complication in the above procedure, which is not usually taken into account, is that in principle apart from the unknown interaction form one has also the ambiguity in the dark-energy equation-of-state parameter. Hence, in the present work we are interested in performing a systematic confrontation of interacting dark energy scenarios, considering however all well-studied parametrizations for the dark-energy equation-of-state parameter. Only such a complete and consistent analysis can extract safe results about the observational validity of the examined scenarios.

We consider interacting scenarios in which the dark energy equation of state is parametrized with forms that include one free parameter. Such one-parameter mod-

*Electronic address: supriya.maths@presiuniv.ac.in
†Electronic address: d11102004@163.com
‡Electronic address: eleonora.divalentino@manchester.ac.uk
§Electronic address: msaridak@phys.uoa.gr
¶Electronic address: schakraborty.math@gmail.com

els are more economical comparing to the two-parameter ones, and moreover recently it was found that these one-parameter dynamical dark-energy parametrizations are very efficient in alleviating the H_0 tension in the simple non-interacting framework [83]. This motivates us to consider a wider picture in which the interaction should be allowed too, and to check whether the H_0 tension is still released, since it has been argued that an allowance of a non-gravitational interaction between dark matter and dark energy naturally increases the error bars on H_0 (due to the existing correlation between H_0 and the coupling parameter of the interaction models) and consequently alleviates the corresponding tension [69, 70, 79, 81]. Thus, essentially the present work aims to investigate whether the release of H_0 tension discussed in [83] is influenced by the presence of an interaction between dark matter and dark energy.

The work has been organized in the following manner. In section II we describe the basic equations for any interacting dark energy model at the background and perturbative levels. Additionally, we present various one-parameter w_x parametrizations. Section III deals with the observational data that we consider in this work. In section IV we describe the main observational results extracted for all the examined scenarios. Moreover, in section V we compute the Bayesian evidences of the models with respect to the reference ΛCDM paradigm. Finally, in section VI we conclude the present work with a brief summary of all findings.

II. COSMOLOGICAL EQUATIONS IN INTERACTING SCENARIOS

The universe is well described by the homogeneous and isotropic Friedman-Lemaître-Robertson-Walker (FLRW) line element given by

$$ds^2 = -dt^2 + a^2(t)\left[\frac{dr^2}{1-Kr^2} + \left(d\theta^2 + \sin^2\theta d\phi^2\right)\right], \quad (1)$$

where $a(t)$ is the expansion scale factor and $K = 0, -1, +1$ corresponds respectively to flat, open and closed spatial geometry. Since observations imply almost spatial flatness, we shall restrict ourselves to $K = 0$ throughout the work.

The total matter content of the universe constitutes to radiation, baryons, pressure-less dark matter and a dark energy fluid (that may be real fluid or an effective one arising from modified gravity). Moreover, we allow the dark matter and dark energy to have a mutual (non-gravitational) interaction, while the remaining two fluids follow the usual conservation laws. Hence, the Friedmann equation is given by

$$H^2 = \frac{8\pi G}{3}\left(\rho_r + \rho_b + \rho_c + \rho_x\right), \quad (2)$$

in which $H \equiv \dot{a}/a$ is the Hubble rate, and ρ_i is the energy density of the i-th fluid sector (with $i = r$ for radiation, $i = b$ for baryons, $i = c$ for cold or pressure-less dark matter and $i = x$ for dark energy). The conservation equation of the total fluid $\rho_{\rm tot} = \rho_r + \rho_b + \rho_c + \rho_x$, is given by

$$\dot{\rho}_{\rm tot} + 3H\left(\rho_{\rm tot} + p_{\rm tot}\right) = 0, \quad (3)$$

where $p_{\rm tot}$ is the total pressure of the fluids defined as $p_{\rm tot} = p_r + p_b + p_c + p_x$. Since radiation and baryons satisfy their own conservation equations, namely, $\dot{\rho}_b + 3H\rho_b = 0$ and $\dot{\rho}_r + 4H\rho_r = 0$, then the conservation equation for the total fluid (3) gives rise to

$$\dot{\rho}_{\rm Dark} + 3H\left(p_{\rm Dark} + \rho_{\rm Dark}\right) = 0, \quad (4)$$

where $\rho_{\rm Dark} = \rho_c + \rho_x$ and $p_{\rm Dark} = p_c + p_x$.

In interacting cosmology one splits the conservation equation for the dark sector (4) into

$$\dot{\rho}_c + 3H\rho_c = -Q(t), \quad (5)$$

and

$$\dot{\rho}_x + 3H(1+w_x)\rho_x = Q(t), \quad (6)$$

by introducing a new function $Q(t)$, that actually characterizes the rate of energy transfer between these dark fluids. Thus, whenever the interaction Q is prescribed, using the conservation equations (5), (6) as well as the Friedmann equation (2), one can determine the dynamics of this interacting scenario.

Since the nature of both dark fluids is unknown, there is an ambiguity in the choice of the interaction function. Thus, in general one considers phenomenological choices for Q, and through observational confrontation results to the best interaction model. In the present work we will focus on a well motivated interaction that induces stable perturbations [99]:

$$Q = 3\xi H(1+w_x)\rho_x, \quad (7)$$

with ξ the coupling parameter characterizing the interaction strength.

Let us briefly describe the perturbation equations for an interacting dark energy model following [100, 101, 102]. The scalar perturbations of the FLRW metric read as

$$ds^2 = a^2(\tau)\Bigg[-(1+2\phi)d\tau^2 + 2\partial_i B d\tau dx^i + \Big((1-2\psi)\delta_{ij} + 2\partial_i\partial_j E\Big)dx^i dx^j\Bigg], \quad (8)$$

where τ is the conformal time and the ϕ, B, ψ and E are the gauge-dependent scalar perturbation quantities. Additionally, for an interacting universe the conservation equations become [103, 104, 105]

$$\nabla_\nu T^{\mu\nu}_A = Q^\mu_A, \qquad \sum_{\rm A} Q^\mu_A = 0, \quad (9)$$

where A is used to represent either pressure-less dark matter (then $A = c$) or dark energy (then $A = x$). Here, the quantity Q^{μ}_{A} takes the following expression

$$Q^{\mu}_{A} = (Q_A + \delta Q_A)u^{\mu} + a^{-1}(0, \partial^i f_A), \tag{10}$$

relative to the four-velocity u^{μ}, in which Q_A presents the background energy transfer (i.e. $Q_A = Q$) and f_A is the momentum transfer potential. We restrict ourselves to the simplest possibility following the earlier works [103, 104, 105], i.e. we assume that the momentum transfer potential is zero in the rest frame of the dark matter, from which one can derive that $k^2 f_A = Q_A(\theta - \theta_c)$ (here k is the wave number; $\theta = \theta^{\mu}_{\mu}$ is the volume expansion scalar of the total fluid, and θ_c is the the volume expansion scalar for the CDM fluid).

We proceed by applying the synchronous gauge to derive the perturbation equations for the interacting scenarios. Thus, in the synchronous gauge we have $\phi = B = 0$, $\psi = \eta$, and $k^2 E = -h/2 - 3\eta$ (h and η are the metric perturbations, see [101] for details). Additionally, we assume the absence of an anisotropic stress, and we define the density perturbations for the fluid A by $\delta_A = \delta\rho_A/\rho_A$. The resulting perturbation equations become

$$\begin{aligned}
\delta'_x &= -(1+w_x)\left(\theta_x + \frac{h'}{2}\right) - 3\mathcal{H}w'_x\frac{\theta_x}{k^2} \\
&\quad -3\mathcal{H}(c^2_{sx} - w_x)\left[\delta_x + 3\mathcal{H}(1+w_x)\frac{\theta_x}{k^2}\right] \\
&\quad +\frac{aQ}{\rho_x}\left[-\delta_x + \frac{\delta Q}{Q} + 3\mathcal{H}(c^2_{sx} - w_x)\frac{\theta_x}{k^2}\right], \quad (11) \\
\theta'_x &= -\mathcal{H}(1 - 3c^2_{sx})\theta_x + \frac{c^2_{sx}}{(1+w_x)}k^2\delta_x \\
&\quad +\frac{aQ}{\rho_x}\left[\frac{\theta_c - (1+c^2_{sx})\theta_x}{1+w_x}\right], \quad (12) \\
\delta'_c &= -\left(\theta_c + \frac{h'}{2}\right) + \frac{aQ}{\rho_c}\left(\delta_c - \frac{\delta Q}{Q}\right), \quad (13) \\
\theta'_c &= -\mathcal{H}\theta_c, \quad (14)
\end{aligned}$$

where $\mathcal{H} = aH$ is the conformal Hubble rate and in (11), (12), (13) the factor $\delta Q/Q$ incorporates the perturbations for the Hubble rate δH. We mention that using δH one can easily find the gauge invariant perturbation equations [17].

We close this section by introducing the w_x parametrizations having only one free parameter w_0, namely the present value of the dark energy equation of state [83]:

$$\begin{aligned}
&\text{Model I}: \quad w_x(a) = w_0 a[1 - \log(a)], \quad (15) \\
&\text{Model II}: \quad w_x(a) = w_0 a \exp(1-a), \quad (16) \\
&\text{Model III}: \quad w_x(a) = w_0 a[1 + \sin(1-a)], \quad (17) \\
&\text{Model IV}: \quad w_x(a) = w_0 a[1 + \arcsin(1-a)]. \quad (18)
\end{aligned}$$

Thus, in summary we consider the interaction model (7) with four different dark energy equations of state given in (15)-(18). From now on we identify the interaction model (7) with w_x of (15) as IDE1, interaction model (7) with (16) as IDE2, interaction model (7) with (17) as IDE3, and finally the interaction model (7) with (18) as IDE4.

III. OBSERVATIONAL DATA

In this section we describe the observational data that we use to investigate the interacting dark energy models, and we provide a brief description on the methodology.

- The data from cosmic microwave background (CMB) observations are very powerful to analyze the cosmological models. Here we use the high-ℓ temperature and polarization as well as the low-ℓ temperature and polarization 2015 CMB angular power spectra from the Planck experiment (Planck TT, TE, EE + lowTEB) [106, 107].
- We include the Joint light-curve analysis (JLA) sample from Supernovae Type Ia data [108].
- We use the Baryon acoustic oscillations (BAO) distance measurements from the following references [109, 110, 111].
- We consider the measurements of the Hubble parameter at various redshifts from the Cosmic Chronometers (CC) [112].
- We adopt a gaussian prior on the Hubble constant (R19) $H_0 = 74.02 \pm 1.42$ as obtained from SH0ES [113].

Parameter	Prior
$\Omega_b h^2$	$[0.005, 0.1]$
$\Omega_c h^2$	$[0.01, 0.99]$
τ	$[0.01, 0.8]$
n_s	$[0.5, 1.5]$
$\log[10^{10} A_s]$	$[2.4, 4]$
$100\theta_{MC}$	$[0.5, 10]$
w_0	$[-2, 0]$
ξ	$[0, 2]$

TABLE I: The table shows the priors imposed on various free parameters of the interacting scenarios during the statistical analysis.

In order to extract the observational constraints on the model parameters of the interaction scenarios, we use the efficient cosmological code `cosmomc` [114, 115], a markov chain monte carlo package which (i) has a convergence diagnostic and (ii) supports the Planck 2015

Parameters	CMB	CMB+BAO	CMB+BAO+JLA	CMB+BAO+JLA+CC	CMB+R19	CMB+BAO+R19
$\Omega_c h^2$	$0.1209^{+0.0015+0.0038}_{-0.0020-0.0035}$	$0.1194^{+0.0013+0.0025}_{-0.0013-0.0025}$	$0.1187^{+0.0012+0.0023}_{-0.0012-0.0022}$	$0.1187^{+0.0012+0.0025}_{-0.0012-0.0025}$	$0.1202^{+0.0015+0.0028}_{-0.0016-0.0027}$	$0.1198^{+0.0012+0.0024}_{-0.0012-0.0024}$
$\Omega_b h^2$	$0.02220^{+0.00016+0.00031}_{-0.00015-0.00031}$	$0.02223^{+0.00016+0.00028}_{-0.00015-0.00029}$	$0.02226^{+0.00014+0.00028}_{-0.00014-0.00027}$	$0.02226^{+0.00014+0.00028}_{-0.00014-0.00028}$	$0.02219^{+0.00015+0.00028}_{-0.00015-0.00028}$	$0.02222^{+0.00015+0.00030}_{-0.00016-0.00031}$
$100\theta_{MC}$	$1.04036^{+0.00037+0.00065}_{-0.00031-0.00070}$	$1.04049^{+0.00032+0.00063}_{-0.00032-0.00065}$	$1.04058^{+0.00030+0.00060}_{-0.00030-0.00058}$	$1.04059^{+0.00029+0.00059}_{-0.00031-0.00060}$	$1.04040^{+0.00035+0.00056}_{-0.00032-0.00060}$	$1.04044^{+0.00033+0.00062}_{-0.00033-0.00060}$
τ	$0.080^{+0.018+0.035}_{-0.018-0.035}$	$0.086^{+0.018+0.036}_{-0.018-0.036}$	$0.092^{+0.017+0.034}_{-0.018-0.034}$	$0.092^{+0.018+0.033}_{-0.017-0.034}$	$0.081^{+0.017+0.034}_{-0.019-0.032}$	$0.082^{+0.018+0.037}_{-0.018-0.037}$
n_s	$0.9734^{+0.0044+0.0081}_{-0.0044-0.0082}$	$0.9748^{+0.0042+0.0084}_{-0.0041-0.0082}$	$0.9764^{+0.0041+0.0081}_{-0.0040-0.0079}$	$0.9766^{+0.0041+0.0088}_{-0.0042-0.0083}$	$0.9734^{+0.0047+0.0082}_{-0.0047-0.0083}$	$0.9739^{+0.0040+0.0083}_{-0.0041-0.0077}$
$\ln(10^{10}A_s)$	$3.103^{+0.034+0.067}_{-0.034-0.067}$	$3.114^{+0.037+0.070}_{-0.034-0.069}$	$3.124^{+0.034+0.067}_{-0.035-0.065}$	$3.124^{+0.036+0.065}_{-0.033-0.065}$	$3.107^{+0.033+0.068}_{-0.037-0.068}$	$3.108^{+0.035+0.072}_{-0.034-0.072}$
w_0	$< -1.30\ < -1.07$	$-1.207^{+0.058+0.11}_{-0.054-0.11}$	$-1.137^{+0.037+0.074}_{-0.037-0.073}$	$-1.138^{+0.041+0.082}_{-0.040-0.085}$	$-1.306^{+0.053+0.09}_{-0.046-0.10}$	$-1.263^{+0.041+0.089}_{-0.040-0.088}$
ξ	$< 0.0068\ < 0.014$	$< 0.0047\ < 0.0071$	$0.0030^{+0.0019}_{-0.0020}\ < 0.0058$	$0.0031^{+0.0019}_{-0.0021}\ < 0.0059$	$< 0.0061\ < 0.0088$	$< 0.0054\ < 0.0080$
Ω_{m0}	$0.231^{+0.077+0.109}_{-0.081-0.098}$	$0.283^{+0.011+0.022}_{-0.011-0.022}$	$0.297^{+0.0087+0.0171}_{-0.0088-0.0169}$	$0.296^{+0.0088+0.0175}_{-0.0086-0.0176}$	$0.2632^{+0.0095+0.020}_{-0.0095-0.020}$	$0.271^{+0.0077+0.016}_{-0.0074-0.016}$
σ_8	$0.932^{+0.087+0.144}_{-0.090-0.143}$	$0.855^{+0.021+0.040}_{-0.021-0.038}$	$0.835^{+0.018+0.034}_{-0.017-0.034}$	$0.836^{+0.017+0.035}_{-0.017-0.033}$	$0.882^{+0.018+0.034}_{-0.020-0.033}$	$0.870^{+0.019+0.032}_{-0.017-0.035}$
H_0	81^{+13+17}_{-14-16}	$71.0^{+1.5+2.9}_{-1.5-3.0}$	$69.1^{+1.0+2.0}_{-1.0-2.0}$	$69.2^{+1.0+2.1}_{-1.1-2.1}$	$73.8^{+1.2+3.0}_{-1.5-2.6}$	$72.6^{+1.0+2.2}_{-1.0-2.0}$
S_8	$0.820^{+0.038+0.061}_{-0.045-0.08}$	$0.824^{+0.019+0.035}_{-0.017-0.055}$	$0.823^{+0.020+0.036}_{-0.017-0.057}$	$0.825^{+0.017+0.034}_{-0.015-0.051}$	$0.826^{+0.026+0.031}_{-0.016-0.030}$	$0.826^{+0.015+0.030}_{-0.016-0.030}$

TABLE II: 68% and 95% confidence-level constraints on the interacting scenario IDE1 with the dark energy equation of state $w_x(a) = w_0 a[1 - \log(a)]$ (Model I) for various observational datasets. Here Ω_{m0} is the present value of the total matter density parameter $\Omega_m = \Omega_b + \Omega_c$, and H_0 is in units of km/sec/Mpc.

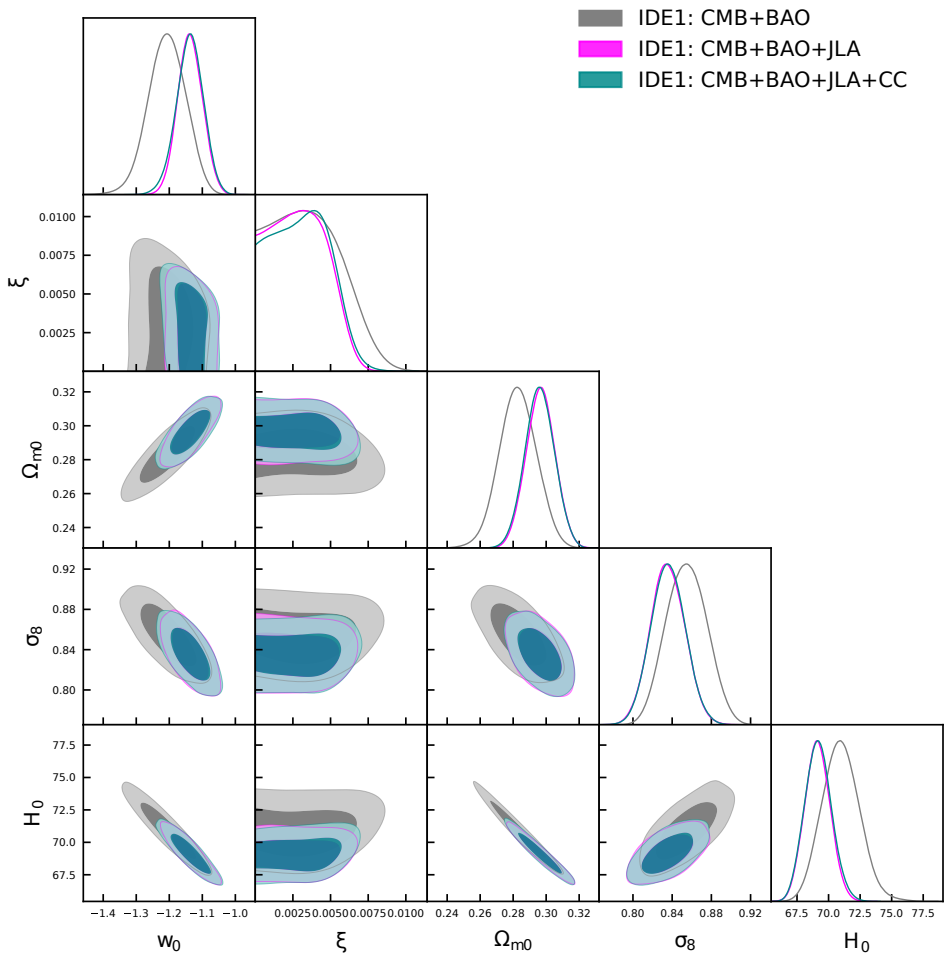


FIG. 1: *The 68% and 95% Confidence Level (CL) contour plots between various combinations of the model parameters of scenario IDE1, using different observational astronomical datasets. Additionally we display the one-dimensional marginalized posterior distributions of some free parameters.*

likelihood code [107]. The dimension of the parameters space for all interaction scenarios is eight, where $\mathcal{P} \equiv \left\{\Omega_b h^2, \Omega_c h^2, 100\theta_{MC}, \tau, w_0, \xi, n_s, log[10^{10} A_S]\right\}$. Here $\Omega_b h^2$ is the physical baryon density, $\Omega_c h^2$ is the physical density for cold dark matter, $100\theta_{MC}$ denotes the ratio of the sound horizon to the angular diameter distance, τ denotes the reionization optical depth, n_s is

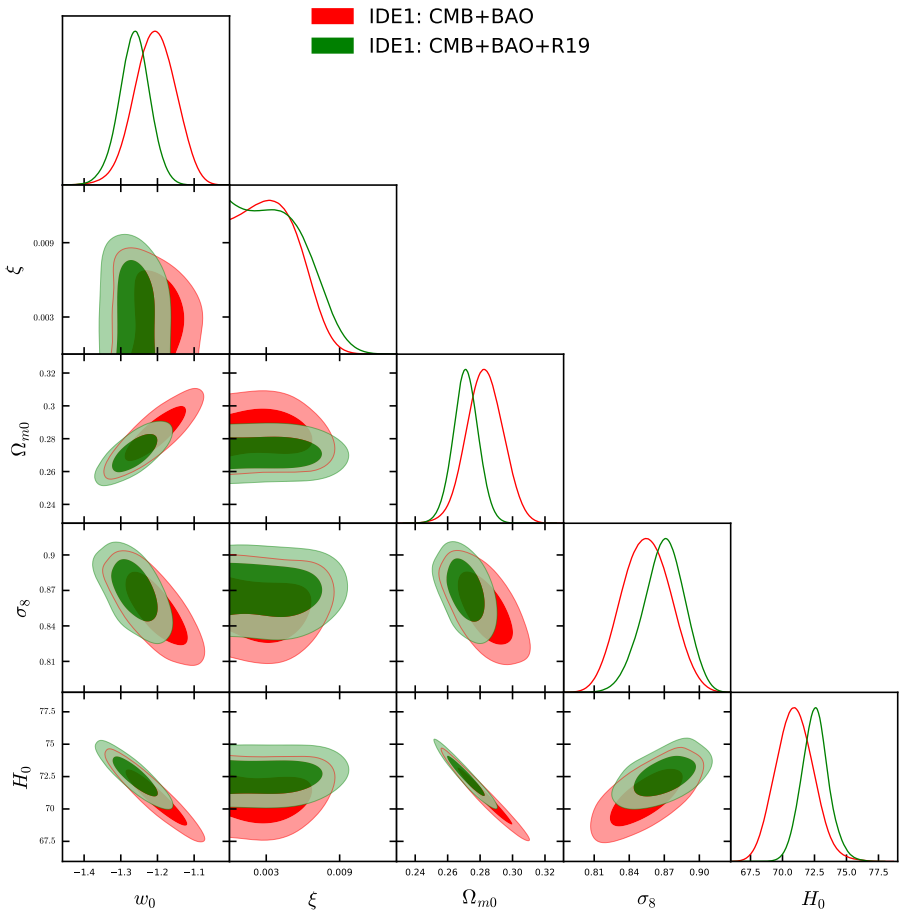


FIG. 2: *The 68% and 95% CL contour plots between various combinations of the model parameters of scenario IDE1 using only the CMB+BAO and CMB+BAO+R19 datasets, and the corresponding one-dimensional marginalized posterior distributions.*

the scalar spectral index, A_S is the amplitude of the primordial scalar power spectrum, w_0 is the current value of the dark energy parameter, and ξ is the coupling parameter of the interaction. In Table I we summarize the flat priors on the model parameters during the statistical analysis.

IV. RESULTS AND IMPLICATIONS

In this section we extract the observational constraints on the present four interacting dark energy scenarios where dark energy has a time-dependent equation-of-state parameter. For all interacting scenarios we have performed several analyses using the observational data described in section III.

A. IDE1: Interacting dark energy with $w_x = w_0 a[1 - \log(a)]$

The summary of the observational constraints for this interaction scenario using different observational datasets is presented in Table II, while the 2-D contour plots and the 1-D marginalized posterior distribution are shown in Figs. 1 and 2. We mention that in the figures we do not include the sole CMB case, since its parameter space is larger than the other datasets, however we note that the qualitative nature of the correlations between the parameters for CMB alone and other cases are similar. Moreover, we notice that the addition of CC to the CMB+BAO+JLA combination does not add extra constraining power, and hence the constraints from CMB+BAO+JLA and CMB+BAO+JLA+CC are actually the same in the fourth and fifth columns of Table II.

From the results we observe that for both CMB and CMB+BAO $\xi = 0$ is consistent within 68% CL. After the inclusion of JLA and JLA+CC to the combined dataset CMB+BAO, we find that an interaction of about $\xi = 0.003 \pm 0.002$ is suggested at 68% CL. In addition, if we combine CMB with R19 (we can safely do it since the tension on H_0 is less than 2σ as we can see in Fig. 3) we find an improved constraint (statistically very mild) but always in agreement with $\xi = 0$, while combining CMB+BAO+R19 gives slightly relaxed constraints Therefore, we conclude that for

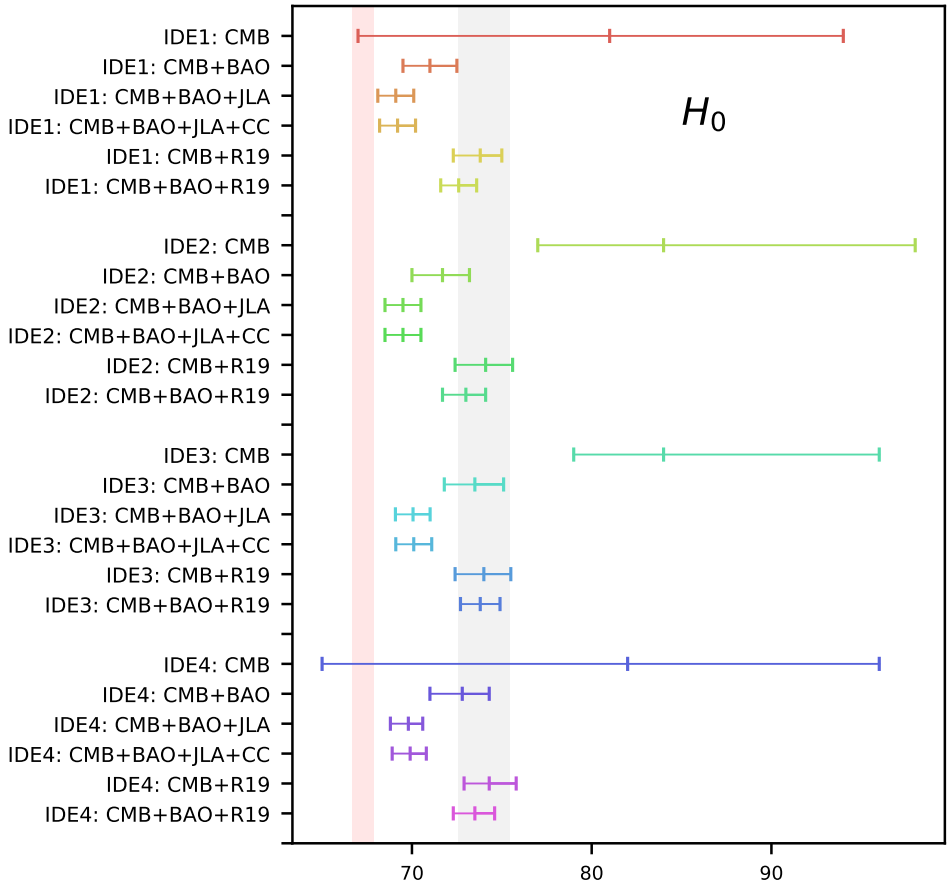


FIG. 3: *Whisker plot with the 68% CL constraints on the Hubble constant for all interacting models and all combination of datasets considered in this work. The grey vertical band corresponds to the R19 value for the Hubble constant, H_0, as measured by SH0ES in [113], and the red vertical band is the one estimate by the Planck 2018 release [116].*

CMB+BAO+JLA, CMB+BAO+JLA+CC, CMB+R19 and CMB+BAO+R19, $\xi \neq 0$ at 1σ, however within 95% CL, ξ is consistent with zero.

Concerning the current value of the dark energy equation of state w_0, for all combination of datasets it always lies in the phantom regime at more than two/three standard deviations. If we compare these results with those without interaction obtained in [83], we see that they are perfectly in agreement and very robust, even in those cases where an interaction different from zero is favoured.

Regarding the estimated values of Ω_{m0}, one can clearly see that for CMB alone case, Ω_{m0} is really small compared to what Planck estimates [117]. This is due to the geometrical degeneracy existing between w_0, $\Omega_{m,0}$ and H_0. Since a phantom dark energy equation of state is preferred by the Planck data, the position of the peaks in the high multipoles damping tail will be shifted, and we need a lower value for the matter density and an higher Hubble constant to put them back in the measured position. When BAO data are added to CMB, the mean value of Ω_{m0} increases with reduced error bars, because this dataset fixes very well the amount of matter density in the universe. For this reason, all the other dataset combinations we considered have Ω_{m0} greater than the CMB alone case, even if always lower than the Planck one [117].

Finally, concerning the estimation of H_0, we see that for CMB data alone it takes a very high mean value compared to the ΛCDM-based Planck's estimation [116] and the error bars are quite large (as one can see $H_0 = 81^{+13}_{-14}$ at 68% CL for CMB alone). This is an implication of the strong anti-correlation between w_0 and H_0. How-

ever, when the BAO data are added to CMB, the error bars on H_0 are significantly decreased and its estimated mean value shifts towards a lower value ($H_0 = 71.0 \pm 1.5$ at 68% CL for CMB+BAO), i.e. perfectly in agreement with the direct measurements [113, 118, 119] within 2σ. The inclusion of JLA (or JLA+CC) to CMB+BAO further decreases the error bars on H_0 and further shifts its lower value, increasing the H_0 tension, but still less than 3σ.

B. IDE2: Interacting dark energy with $w_x(a) = w_0 a \exp(1-a)$

The observational summary for this interaction scenario is displayed in Table III, while the 2-D contour plots and 1-D parameter distributions are shown in Figs. 4 and 5. From the analyses we deduce that for CMB data alone the non-interacting case $\xi = 0$ is consistent within 68% CL, however when BAO data are added to CMB then an indication of interaction is found at more than 68% CL. Surprisingly when JLA data are added to the previous dataset CMB+BAO, then we again find that $\xi = 0$ consistent within 68% CL. Moreover, for the remaining datasets the indication of an interaction is still present at more than 1σ. We note that due to the addition of R19 with CMB and CMB+BAO, slight improvements in the coupling parameter ξ are observed, although such improvements are statistically very mild. In fact, R19 sets a lower bound on ξ for both CMB+R19 and CMB+BAO+R19. The reason is that the inclusion of R19 with CMB and CMB+BAO breaks the degeneracies between H_0 and other cosmological parameters.

Concerning the dark energy equation-of-state parameter at present, for all the datasets a phantom value $w_0 < -1$ is always supported for more than 95% CL. Hence, in summary, as we can from the results, most of the datasets indicate a non-zero interaction together with the existence of a phantom dark energy. A similar observation on the estimated values of Ω_{m0}, specially for its lower value for CMB alone analysis, is found as in IDE1.

Regarding the estimations of the Hubble parameter H_0, we see that for CMB alone H_0 acquires a very high value with very large error bars compared to the Planck one within minimal ΛCDM model [116] (in particular $H_0 = 84^{+14}_{-7}$ at 68% CL with CMB alone). This is due to the strong correlation between w_0 and H_0. When external datasets are added, as for instance BAO, JLA, CC, R19, and their combinations, the estimations of H_0 decrease with significant reduction in the error bars, but they can still relieve the tension with [113] within 3 standard deviations.

C. IDE3: Interacting dark energy with $w_x(a) = w_0 a[1 + \sin(1-a)]$

The summary of the observational constraints for this interaction scenario using different observational datasets is presented in Table IV and in Figs. 6 and 7 we show the 2-D contour plots and 1-D posterior distributions for some of the free parameters and dataset combinations.

Concerning the coupling parameter our analysis reveals some interesting features. In particular, as we can see, for CMB data alone we have $\xi = 0$ within 68% CL and hence it is consistent with a non-interacting cosmology. Nevertheless, as soon as external datasets, namely BAO, JLA, CC or R19 are added in different combinations (such as CMB+BAO, CMB+BAO+JLA, CMB+BAO+JLA+CC and CMB+R19) we see that a non-zero interaction is favoured at more than 1σ. However, we mention that within 95% CL these combinations of observational datasets allow for a non-interacting cosmology. We note that the R19 has similar effects when combined with CMB and CMB+BAO, as already reported previously for IDE2.

Concerning the current value of the dark energy equation of state w_0, we find a similar character to what we already found in IDE1 and IDE2. In particular, the results show that irrespectively of the observational datasets that we have used in this work, w_0 remains less than -1 at more than 95% CL, i.e. in the phantom region, for the CMB only case, and several standard deviations (more than five) for the combinations with the other cosmological probes. If we compare this Table with the results shown in [83] for the same model without interaction, we can see that the constraints are very robust, and only the upper limit of w_0 for the CMB alone case is slightly removed to less phantom values. Furthermore we mention that in this scenario the CC dataset does not improve the constraints at all. Let us note that similar to IDE1 and IDE2, for CMB alone analysis, Ω_{m0} acquires a lower value compared to Planck [117].

Finally, regarding the H_0 parameter we again find a similar behaviour to what we observed for IDE1 and IDE2. Since to a phantom dark energy equation of state corresponds a higher value of the Hubble parameter, due to their negative correlation, the highly negative w_0 values that we obtain are accompanied with a high value of H_0 with large asymmetric error bars. Specifically, we find $H_0 = 84^{+12}_{-5}$ at 68% CL, which is much higher than the recent ΛCDM-based estimation by Planck [116], but in agreement with the direct measurements $H_0 = 73.24 \pm 1.74$ of [118], $H_0 = 73.48 \pm 1.66$ of [119] or $H_0 = 74.03 \pm 1.42$ of [113]. However, after the inclusion of the external datasets such as BAO, JLA, CC and R19 we find that H_0 decreases with respect to its estimation from CMB alone, and additionally its error bars are significantly reduced.

Parameters	CMB	CMB+BAO	CMB+BAO+JLA	CMB+BAO+JLA+CC	CMB+R19	CMB+BAO+R19
$\Omega_c h^2$	$0.1214^{+0.0017+0.0042}_{-0.0022-0.0040}$	$0.1197^{+0.0012+0.0025}_{-0.0012-0.0024}$	$0.1191^{+0.0011+0.0022}_{-0.0011-0.0023}$	$0.1191^{+0.0012+0.0024}_{-0.0012-0.0024}$	$0.12061377^{+0.0015+0.0029}_{-0.0014-0.0039}$	$0.1199^{+0.0012+0.0024}_{-0.0013-0.0023}$
$\Omega_b h^2$	$0.02218^{+0.00016+0.00032}_{-0.00016-0.00034}$	$0.02221^{+0.00014+0.00029}_{-0.00015-0.00026}$	$0.02222^{+0.00014+0.00027}_{-0.00014-0.00027}$	$0.02223^{+0.00014+0.00027}_{-0.00013-0.00026}$	$0.02215^{+0.00014+0.00027}_{-0.00013-0.00026}$	$0.02220^{+0.00014+0.00029}_{-0.00016-0.00028}$
$100\theta_{MC}$	$1.04034^{+0.00035+0.00071}_{-0.00034-0.00072}$	$1.04045^{+0.00031+0.00058}_{-0.00030-0.00060}$	$1.04050^{+0.00034+0.00058}_{-0.00031-0.00060}$	$1.04051^{+0.00032+0.00066}_{-0.00032-0.00065}$	$1.04036^{+0.00034+0.00068}_{-0.00034-0.00073}$	$1.04042^{+0.00030+0.00060}_{-0.00030-0.00060}$
τ	$0.079^{+0.018+0.034}_{-0.018-0.035}$	$0.088^{+0.018+0.034}_{-0.018-0.035}$	$0.095^{+0.016+0.032}_{-0.017-0.033}$	$0.094^{+0.018+0.033}_{-0.017-0.033}$	$0.082^{+0.017+0.033}_{-0.016-0.036}$	$0.086^{+0.017+0.033}_{-0.017-0.033}$
n_s	$0.9729^{+0.0045+0.0089}_{-0.0045-0.0092}$	$0.9748^{+0.0042+0.0084}_{-0.0043-0.0084}$	$0.9762^{+0.0042+0.0082}_{-0.0042-0.0081}$	$0.9764^{+0.0042+0.0079}_{-0.0045-0.0076}$	$0.9723^{+0.0051+0.0098}_{-0.0049-0.0094}$	$0.9741^{+0.0040+0.0084}_{-0.0040-0.0084}$
$\ln(10^{10}A_s)$	$3.103^{+0.035+0.066}_{-0.035-0.070}$	$3.119^{+0.035+0.066}_{-0.034-0.068}$	$3.131^{+0.032+0.066}_{-0.032-0.064}$	$3.129^{+0.033+0.065}_{-0.034-0.067}$	$3.108^{+0.034+0.063}_{-0.031-0.072}$	$3.115^{+0.035+0.065}_{-0.033-0.064}$
w_0	$< -1.53\ < -1.08$	$-1.249^{+0.064+0.12}_{-0.055-0.12}$	$-1.166^{+0.038+0.072}_{-0.038-0.074}$	$-1.168^{+0.041+0.075}_{-0.034-0.081}$	$-1.341^{+0.058+0.09}_{-0.047-0.11}$	$-1.292^{+0.051+0.083}_{-0.042-0.089}$
ξ	$< 0.0071\ < 0.015$	$0.0024^{+0.0015}_{-0.0016}\ < 0.0047$	$< 0.0027\ < 0.0038$	$0.0021^{+0.0014}_{-0.0013}\ < 0.0039$	$0.0024^{+0.0009}_{-0.0021}\ < 0.0053$	$0.0027^{+0.0016}_{-0.0017}\ < 0.0051$
Ω_{m0}	$0.212^{+0.023+0.132}_{-0.071-0.085}$	$0.277^{+0.012+0.022}_{-0.011-0.023}$	$0.295^{+0.0086+0.017}_{-0.0085-0.018}$	$0.294^{+0.0085+0.018}_{-0.0086-0.018}$	$0.261^{+0.011+0.022}_{-0.011-0.022}$	$0.2683^{+0.0076+0.016}_{-0.0081-0.016}$
σ_8	$0.956^{+0.100+0.123}_{-0.044-0.169}$	$0.859^{+0.022+0.043}_{-0.022-0.043}$	$0.835^{+0.017+0.032}_{-0.017-0.033}$	$0.835^{+0.018+0.037}_{-0.018-0.036}$	$0.886^{+0.020+0.037}_{-0.023-0.036}$	$0.872^{+0.020+0.038}_{-0.019-0.038}$
H_0	84^{+14+16}_{-7-21}	$71.7^{+1.5+3.3}_{-1.7-3.1}$	$69.5^{+1.0+2.0}_{-1.0-1.9}$	$69.5^{+1.0+2.0}_{-1.0-1.9}$	$74.1^{+1.5+2.9}_{-1.7-2.8}$	$73.0^{+1.1+2.2}_{-1.3-2.1}$
S_8	$0.811^{+0.045+0.069}_{-0.048-0.078}$	$0.817^{+0.020+0.038}_{-0.017-0.069}$	$0.820^{+0.020+0.037}_{-0.018-0.065}$	$0.819^{+0.020+0.036}_{-0.019-0.060}$	$0.826^{+0.017+0.034}_{-0.016-0.035}$	$0.824^{+0.016+0.030}_{-0.015-0.031}$

TABLE III: 68% and 95% confidence-level constraints on the interacting scenario IDE2 with the dark energy equation of state $w_x(a) = w_0 a \exp(1-a)$ (Model II) for various observational datasets. Here Ω_{m0} is the present value of the total matter density parameter $\Omega_m = \Omega_b + \Omega_c$, and H_0 is in units of km/sec/Mpc.

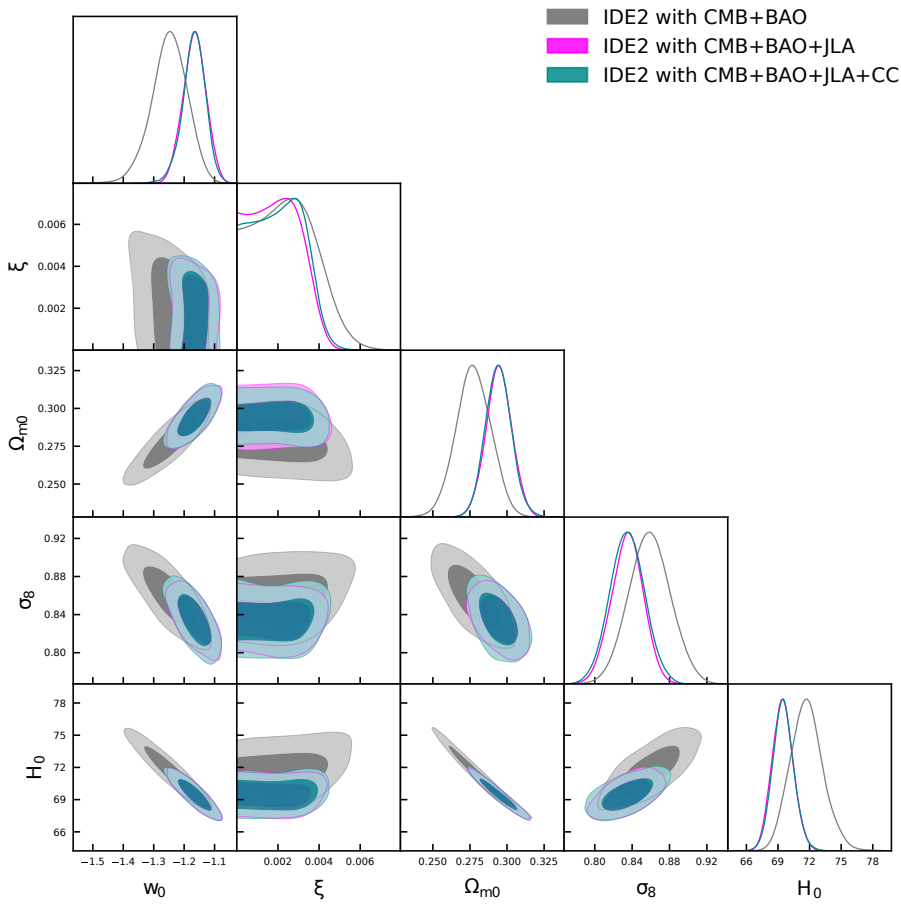


FIG. 4: *The 68% and 95% CL contour plots between various combinations of the model parameters of scenario IDE2, using different observational astronomical datasets. Additionally we display the one-dimensional marginalized posterior distributions of some free parameters.*

In summary, we find that the alleviation of the H_0 tension is more robust in this scenario compared to IDE1 and IDE2 (see also Fig 3). Indeed, one can notice the estimated values of H_0 from different combination of observational datasets as follows:

- CMB+BAO: $H_0 = 73.5^{+1.6}_{-1.7}$ at 68% CL ($H_0 = 73.5 \pm 3.2$ at 95% CL);
- CMB+BAO+JLA: $H_0 = 70.06^{+0.95}_{-0.98}$ at 68% CL ($H_0 = 70.1^{+2.0}_{-1.8}$, at 95% CL);

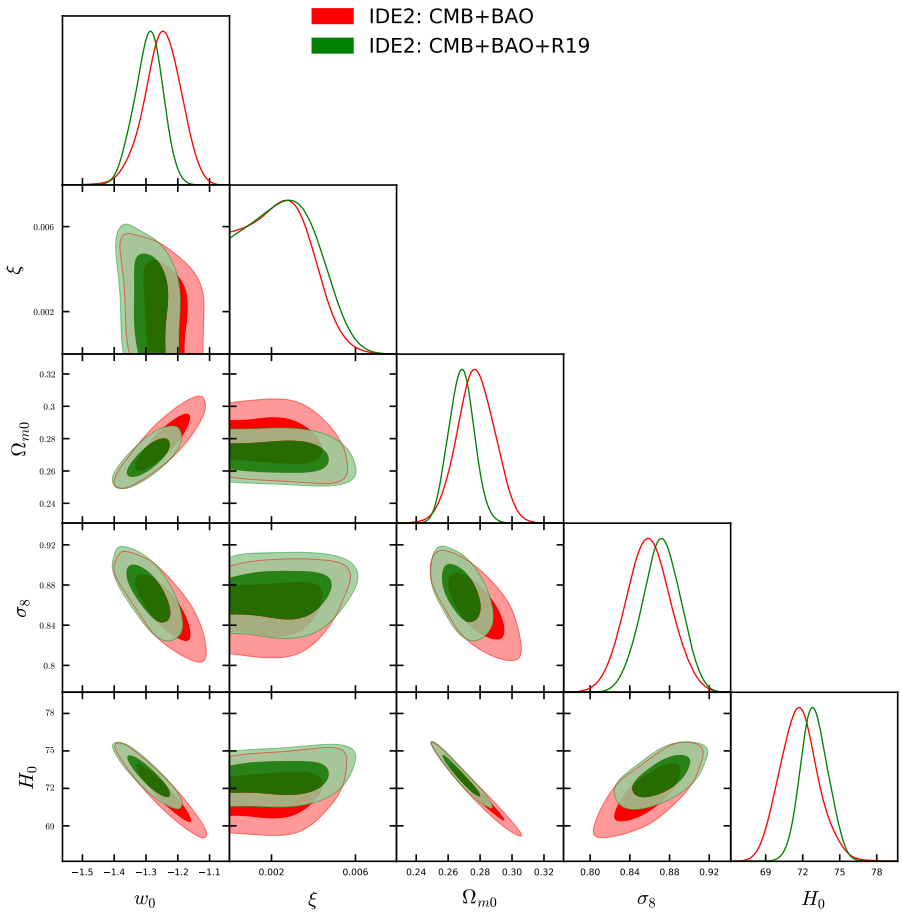


FIG. 5: *The 68% and 95% CL contour plots between various combinations of the model parameters of scenario IDE2 using only the CMB+BAO and CMB+BAO+R19 datasets, and the corresponding one-dimensional marginalized posterior distributions.*

Parameters	CMB	CMB+BAO	CMB+BAO+JLA	CMB+BAO+JLA+CC	CMB+R19	CMB+BAO+R19
$\Omega_c h^2$	$0.1211^{+0.0015+0.0031}_{-0.0015-0.0031}$	$0.1202^{+0.0011+0.0025}_{-0.0013-0.0023}$	$0.1196^{+0.0011+0.0022}_{-0.0012-0.0023}$	$0.1196^{+0.0011+0.0022}_{-0.0012-0.0021}$	$0.1212^{+0.0014+0.0030}_{-0.0016-0.0029}$	$0.1203^{+0.0012+0.0024}_{-0.0013-0.0023}$
$\Omega_b h^2$	$0.02216^{+0.00019+0.00035}_{-0.00016-0.00037}$	$0.02216^{+0.00014+0.00027}_{-0.00014-0.00027}$	$0.02218^{+0.00015+0.00028}_{-0.00016-0.00028}$	$0.02218^{+0.00013+0.00026}_{-0.00013-0.00027}$	$0.02208^{+0.00016+0.00029}_{-0.00016-0.00030}$	$0.02216^{+0.00014+0.00027}_{-0.00014-0.00027}$
$100\theta_{MC}$	$1.04033^{+0.00039+0.00066}_{-0.00035-0.00070}$	$1.04035^{+0.00033+0.00060}_{-0.00030-0.00062}$	$1.04043^{+0.00030+0.00058}_{-0.00030-0.00059}$	$1.04041^{+0.00030+0.00058}_{-0.00029-0.00056}$	$1.04019^{+0.00039+0.00066}_{-0.00036-0.00070}$	$1.04036^{+0.00033+0.00060}_{-0.00030-0.00063}$
τ	$0.079^{+0.017+0.035}_{-0.018-0.035}$	$0.089^{+0.019+0.034}_{-0.017-0.035}$	$0.098^{+0.018+0.036}_{-0.018-0.035}$	$0.098^{+0.017+0.034}_{-0.017-0.033}$	$0.083^{+0.020+0.037}_{-0.020-0.037}$	$0.089^{+0.019+0.033}_{-0.017-0.034}$
n_s	$0.9725^{+0.0046+0.0087}_{-0.0045-0.0086}$	$0.9740^{+0.0040+0.0076}_{-0.0040-0.0080}$	$0.9761^{+0.0042+0.0080}_{-0.0042-0.0080}$	$0.9764^{+0.0039+0.0077}_{-0.0040-0.0077}$	$0.9713^{+0.0044+0.0090}_{-0.0051-0.0082}$	$0.9739^{+0.0040+0.0076}_{-0.0040-0.0081}$
$\ln(10^{10}A_s)$	$3.102^{+0.033+0.068}_{-0.035-0.065}$	$3.120^{+0.037+0.064}_{-0.034-0.068}$	$3.135^{+0.034+0.069}_{-0.035-0.069}$	$3.136^{+0.032+0.065}_{-0.033-0.064}$	$3.111^{+0.040+0.067}_{-0.038-0.068}$	$3.120^{+0.033+0.063}_{-0.033-0.064}$
w_0	< -1.61 < -1.17	$-1.371^{+0.066+0.12}_{-0.058-0.12}$	$-1.246^{+0.040+0.065}_{-0.033-0.072}$	$-1.248^{+0.037+0.065}_{-0.035-0.070}$	$-1.406^{+0.051+0.093}_{-0.053-0.091}$	$-1.380^{+0.044+0.083}_{-0.044-0.084}$
ξ	< 0.0045 < 0.0080	$0.0019^{+0.0011}_{-0.0012} < 0.0036$	$0.0015^{+0.0010}_{-0.0008} < 0.0027$	$0.0015^{+0.0011}_{-0.0008} < 0.0027$	$0.0023^{+0.0014}_{-0.0011} < 0.0039$	$0.0019^{+0.0011}_{-0.0012} < 0.0036$
Ω_{m0}	$0.210^{+0.020+0.12}_{-0.065-0.079}$	$0.265^{+0.012+0.022}_{-0.011-0.022}$	$0.290^{+0.009+0.017}_{-0.009-0.016}$	$0.290^{+0.008+0.016}_{-0.008-0.016}$	$0.263^{+0.011+0.021}_{-0.011-0.020}$	$0.2629^{+0.0078+0.016}_{-0.0078-0.015}$
σ_8	$0.956^{+0.096+0.118}_{-0.039-0.164}$	$0.870^{+0.022+0.044}_{-0.023-0.043}$	$0.831^{+0.017+0.035}_{-0.018-0.034}$	$0.831^{+0.018+0.034}_{-0.018-0.034}$	$0.880^{+0.019+0.040}_{-0.020-0.040}$	$0.873^{+0.018+0.037}_{-0.018-0.036}$
H_0	84^{+12+15}_{-5-19}	$73.5^{+1.6+3.2}_{-1.7-3.2}$	$70.06^{+0.95+2.0}_{-0.98-1.8}$	$70.1^{+1.0+1.9}_{-1.0-1.8}$	$74.0^{+1.5+2.7}_{-1.6-2.8}$	$73.8^{+1.1+2.1}_{-1.1-2.1}$
S_8	$0.807^{+0.045+0.069}_{-0.044-0.074}$	$0.803^{+0.025+0.043}_{-0.021-0.097}$	$0.803^{+0.026+0.043}_{-0.025-0.090}$	$0.800^{+0.028+0.044}_{-0.030-0.090}$	$0.823^{+0.017+0.030}_{-0.016-0.032}$	$0.817^{+0.015+0.030}_{-0.015-0.029}$

TABLE IV: 68% and 95% confidence-level constraints on the interacting scenario IDE3 with the dark energy equation of state $w_x(a) = w_0 a[1 + \sin(1 - a)]$ (Model III) for various observational datasets. Here Ω_{m0} is the present value of the total matter density parameter $\Omega_m = \Omega_b + \Omega_c$, and H_0 is in units of km/sec/Mpc.

- CMB+BAO+JLA+CC: $H_0 = 70.1 \pm 1.0$ at 68% CL ($H_0 = 70.1^{+1.9}_{-1.8}$, at 95% CL),

where the first one is perfectly in agreement with [113], and the last two alleviate the tension at about 2σ.

D. IDE4: Interacting dark energy with $w_x(a) = w_0 a[1 + \arcsin(1 - a)]$

The summary of the observational constraints for this interacting scenario using different observational datasets is displayed in Table V and in Figs. 8 and 9 we present

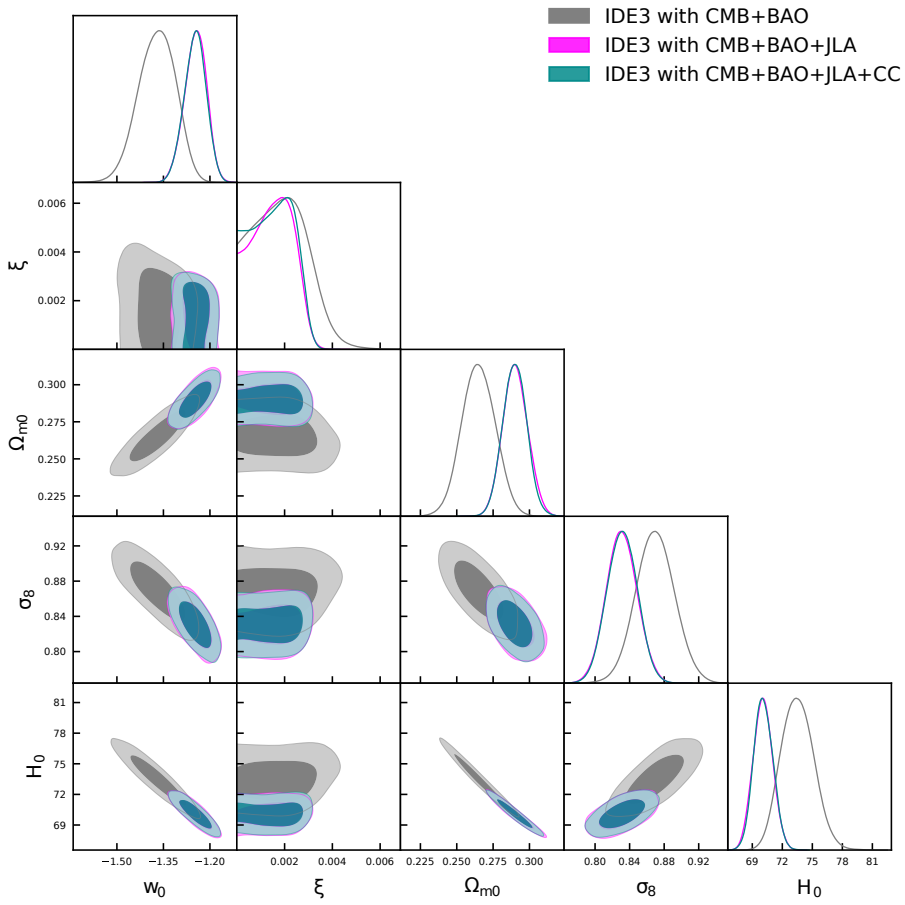


FIG. 6: *The 68% and 95% CL contour plots between various combinations of the model parameters of scenario IDE3, using different observational astronomical datasets. Additionally we display the one-dimensional marginalized posterior distributions of some free parameters.*

Parameters	CMB	CMB+BAO	CMB+BAO+JLA	CMB+BAO+JLA+CC	CMB+R19	CMB+BAO+R19
$\Omega_c h^2$	$0.1212^{+0.0017+0.0034}_{-0.0019-0.0032}$	$0.1200^{+0.0012+0.0026}_{-0.0012-0.0026}$	$0.1192^{+0.0011+0.0022}_{-0.0011-0.0022}$	$0.1193^{+0.0010+0.0022}_{-0.0011-0.0020}$	$0.1208^{+0.0015+0.0022}_{-0.0013-0.0024}$	$0.1201^{+0.0012+0.0026}_{-0.0012-0.0026}$
$\Omega_b h^2$	$0.02214^{+0.00018+0.00034}_{-0.00018-0.00034}$	$0.02217^{+0.00014+0.00027}_{-0.00015-0.00027}$	$0.02222^{+0.00013+0.00029}_{-0.00014-0.00028}$	$0.02222^{+0.00015+0.00027}_{-0.00014-0.00027}$	$0.02212^{+0.00013+0.00028}_{-0.00017-0.00025}$	$0.02217^{+0.00014+0.00027}_{-0.00015-0.00028}$
$100\theta_{MC}$	$1.04027^{+0.00042+0.00076}_{-0.00034-0.00080}$	$1.04040^{+0.00032+0.00062}_{-0.00032-0.00059}$	$1.04046^{+0.00032+0.00056}_{-0.00026-0.00057}$	$1.04050^{+0.00031+0.00059}_{-0.00030-0.00060}$	$1.04027^{+0.00036+0.00057}_{-0.00031-0.00060}$	$1.04040^{+0.00033+0.00060}_{-0.00031-0.00058}$
τ	$0.079^{+0.019+0.032}_{-0.017-0.034}$	$0.089^{+0.018+0.033}_{-0.017-0.034}$	$0.096^{+0.016+0.034}_{-0.016-0.034}$	$0.096^{+0.019+0.036}_{-0.016-0.036}$	$0.077^{+0.025+0.035}_{-0.018-0.038}$	$0.088^{+0.018+0.033}_{-0.017-0.033}$
n_s	$0.9721^{+0.0044+0.0092}_{-0.0047-0.0087}$	$0.9741^{+0.0042+0.0081}_{-0.0042-0.0082}$	$0.9765^{+0.0040+0.0082}_{-0.0044-0.0080}$	$0.9764^{+0.0038+0.0075}_{-0.0038-0.0078}$	$0.9721^{+0.0046+0.0078}_{-0.0036-0.0084}$	$0.9739^{+0.0042+0.0081}_{-0.0042-0.0080}$
$\ln(10^{10}A_s)$	$3.103^{+0.037+0.063}_{-0.031-0.067}$	$3.120^{+0.035+0.066}_{-0.033-0.067}$	$3.132^{+0.034+0.064}_{-0.032-0.064}$	$3.132^{+0.037+0.069}_{-0.032-0.071}$	$3.099^{+0.048+0.067}_{-0.034-0.076}$	$3.118^{+0.035+0.064}_{-0.032-0.066}$
w_0	< -1.48 < -1.02	$-1.331^{+0.067+0.12}_{-0.056-0.13}$	$-1.218^{+0.040+0.067}_{-0.029-0.074}$	$-1.222^{+0.038+0.065}_{-0.033-0.072}$	$-1.394^{+0.045+0.098}_{-0.048-0.092}$	$-1.353^{+0.048+0.084}_{-0.043-0.091}$
ξ	< 0.0041 < 0.0093	< 0.0028 < 0.0042	$0.0017^{+0.0011}_{-0.0011}$ < 0.0032	$0.0018^{+0.0012}_{-0.0011}$ < 0.0033	< 0.0030 < 0.0044	< 0.0030 < 0.0042
Ω_{m0}	$0.229^{+0.098+0.15}_{-0.089-0.096}$	$0.270^{+0.011+0.023}_{-0.012-0.022}$	$0.2919^{+0.0078+0.016}_{-0.0080-0.016}$	$0.291^{+0.0079+0.016}_{-0.0080-0.016}$	$0.260^{+0.011+0.024}_{-0.011-0.023}$	$0.2648^{+0.0078+0.016}_{-0.0080-0.015}$
σ_8	$0.93^{+0.12+0.14}_{-0.14-0.18}$	$0.867^{+0.023+0.046}_{-0.023-0.045}$	$0.832^{+0.016+0.034}_{-0.018-0.032}$	$0.834^{+0.017+0.034}_{-0.017-0.033}$	$0.881^{+0.024+0.039}_{-0.020-0.043}$	$0.874^{+0.019+0.038}_{-0.019-0.037}$
H_0	82^{+14+16}_{-17-21}	$72.8^{+1.5+3.3}_{-1.8-3.0}$	$69.8^{+0.8+1.9}_{-1.0-1.8}$	$69.9^{+0.9+2.0}_{-1.0-1.8}$	$74.3^{+1.5+3.1}_{-1.4-3.2}$	$73.5^{+1.1+2.2}_{-1.2-2.1}$
S_8	$0.818^{+0.041+0.065}_{-0.045-0.074}$	$0.812^{+0.022+0.039}_{-0.019-0.066}$	$0.808^{+0.022+0.040}_{-0.022-0.073}$	$0.810^{+0.022+0.038}_{-0.021-0.070}$	$0.820^{+0.017+0.036}_{-0.018-0.040}$	$0.821^{+0.016+0.032}_{-0.016-0.033}$

TABLE V: 68% and 95% confidence-level constraints on the interacting scenario IDE4 with the dark energy equation of state $w_x(a) = w_0 a[1 + \arcsin(1-a)]$ (Model IV) for various observational datasets. Here Ω_{m0} is the present value of the total matter density parameter $\Omega_m = \Omega_b + \Omega_c$, and H_0 is in units of km/sec/Mpc.

the 2-D contour plots and the 1-D posterior distributions. The behaviour of this interaction scenario has some similarities to that of IDE1. Looking at the results we find also in this case that for the analysis with CMB only and CMB+BAO datasets, the coupling parameter is consistent with $\xi = 0$ within the 68% CL. The addition of JLA or CC, namely the combinations of datasets CMB+BAO+JLA and CMB+BAO+JLA+CC, gives instead an indication for $\xi \neq 0$ at more than 68% CL, but always in agreement with zero within 2σ. We

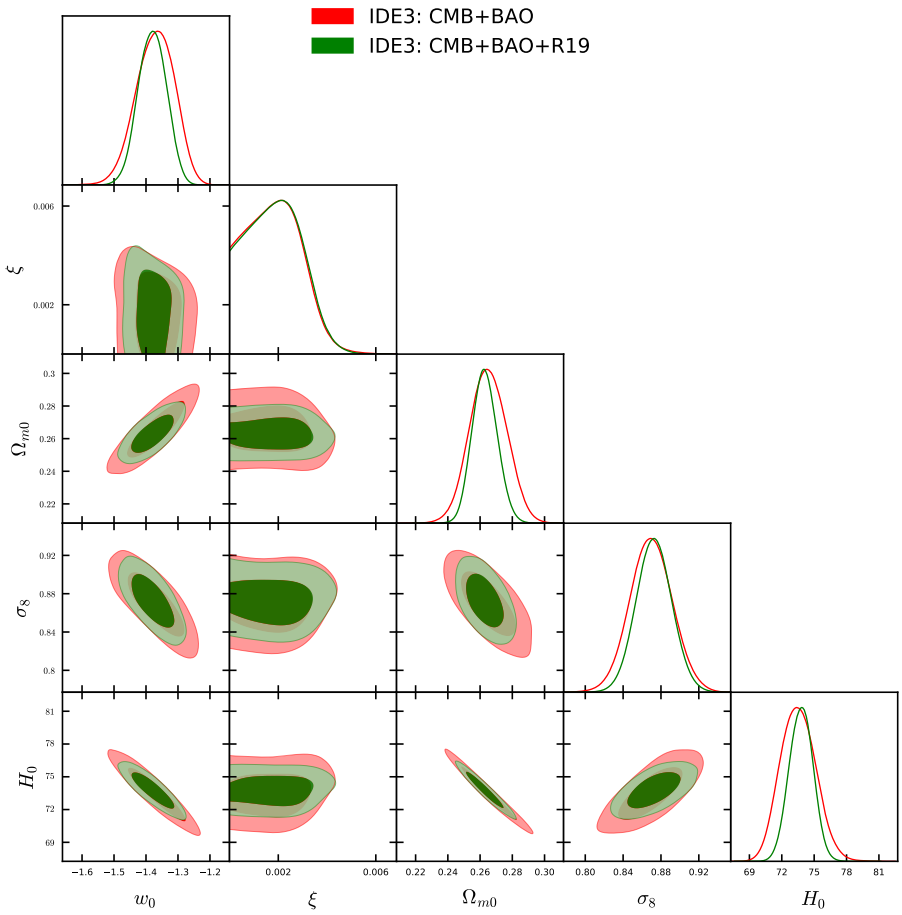


FIG. 7: *The 68% and 95% CL contour plots between various combinations of the model parameters of scenario IDE3 using only the CMB+BAO and CMB+BAO+R19 datasets, and the corresponding one-dimensional marginalized posterior distributions.*

mention that similarly to the previous IDE1 scenarios, here we also see that the inclusion of R19 with CMB and CMB+BAO improves the constraints on ξ, however it gives just an upper bound on it.

Concerning the dark energy equation-of-state parameter at present we extract similar conclusion to the previous interacting scenarios IDE3, namely here too we find that $w_0 < -1$ at more than 95% CL for the CMB only case, and several standard deviations for its combination with the external datasets. Furthermore, for this scenario the CMB only case has a slightly less phantom w_0 than the same case without interaction, as can be seen in [83]. As already reported in earlier IDE models, Ω_{m0} for CMB alone case obtains a lower value, contrary to Planck observations [117].

Now we focus on the trend on the Hubble parameter H_0. For the datasets we use, in this case it is again anti-correlated with w_0, as we can see in Fig. 8. We note that similar to the previous interaction scenarios, the CMB only fit returns very high value of H_0 with large error bars, that are reduced after the inclusion of the external datasets such as BAO, JLA and CC. For this scenario we also conclude that the tension with the direct measurements [113, 118, 119] is solved for CMB and CMB+BAO cases, while with the addition of JLA and JLA+CC it is at about 2σ. For this reason we can safely add the R19 measurement to the CMB and CMB+BAO, and we show the results in the last two columns of Table V.

V. BAYESIAN EVIDENCE

In this section we compute the Bayesian evidences of all the examined interacting models in order to compare their observational soundness with respect to some reference model, and in particular with ΛCDM cosmology. We use the publicly available code `MCEvidence` [120, 121] for computing the evidences, since the code directly accepts the MCMC chains of the analysis. We refer to Ref. [83] for the discussions on Bayesian evidence analysis, and in Table VI we provide the revised Jeffreys scale by Kass and Raftery [122].

For all the examined scenarios we compute the values of $\ln B_{ij}$, which are summarized in Table VII. From this Table one can see that ΛCDM paradigm is most of the time preferred over the present IDE models, with

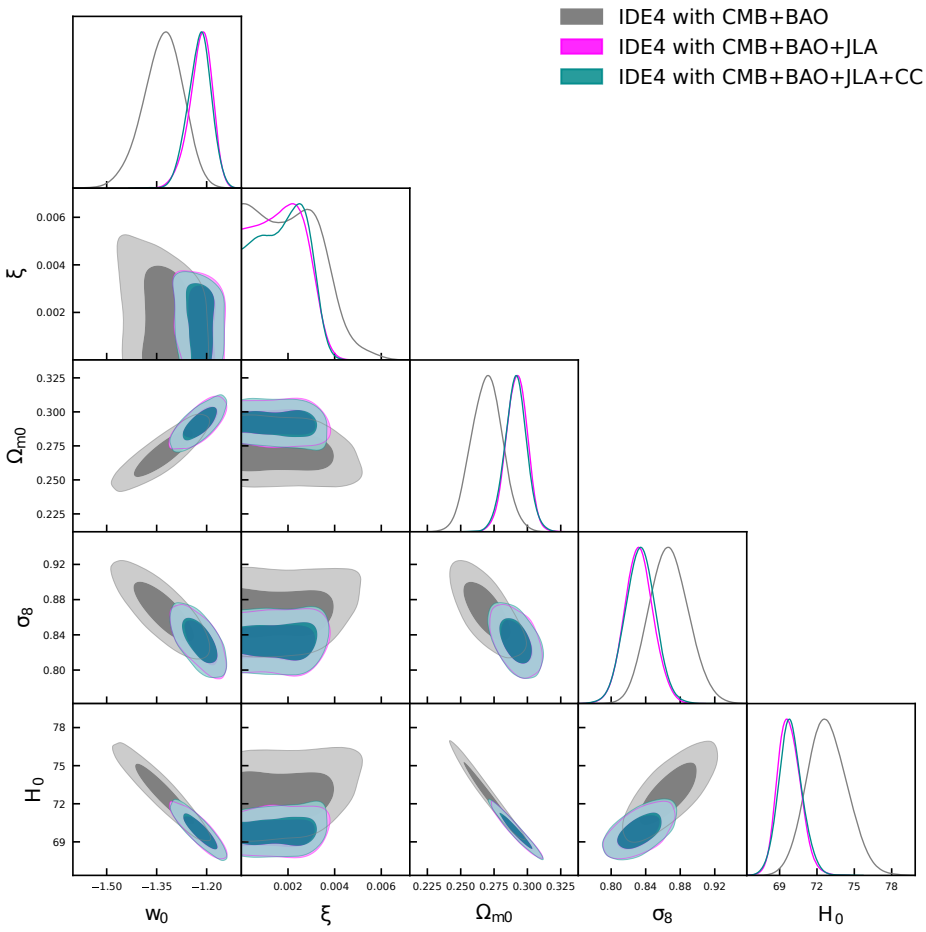


FIG. 8: *The 68% and 95% CL contour plots between various combinations of the model parameters of scenario IDE4, using different observational astronomical datasets. Additionally we display the one-dimensional marginalized posterior distributions of some free parameters.*

$\ln B_{ij}$	Strength of evidence for model M_i
$0 \leq \ln B_{ij} < 1$	Weak
$1 \leq \ln B_{ij} < 3$	Definite/Positive
$3 \leq \ln B_{ij} < 5$	Strong
$\ln B_{ij} \geq 5$	Very strong

TABLE VI: Revised Jeffreys scale [122] that quantifies the comparison of the models.

the exception of the CMB+R19 combination, where we see a weak/positive evidence for all IDE models against ΛCDM. This is expected since the number of free parameters of all IDE models is eight, namely two more compared to the six parameters ΛCDM.

VI. CONCLUDING REMARKS

Interacting scenarios have attracted the interest of the literature, since they are efficient in alleviating the coincidence problem, and additionally they seem to alleviate the H_0 tension and σ_8 tensions. In the present work we investigated interacting scenarios which belong to a wider class, since they include a dynamical dark energy component whose equation of state follows various one-parameter parametrizations. In particular, our focus was to see if a non-zero interaction is favoured, and if the H_0 tension is still alleviated.

We considered a well known interaction in the literature of the form $Q = 3H\xi(1 + w_x)\rho_x$, and we took the dark energy equation-of-state parameter w_x to have the expressions: $w_x(a) = w_0 a[1-\log(a)]$ (Model IDE1), $w_x = w_0 a \exp(1-a)$ (Model IDE2), $w_x(a) = w_0 a[1+\sin(1-a)]$ (Model IDE3), and $w_x(a) = w_0 a[1+\arcsin(1-a)]$ (Model IDE4). Additionally, we used the latest observational data from CMB, JLA, BAO, Hubble parameter measurements from CC, and a gaussian prior on H_0 labeled as R19 from SH0ES [113].

Our analysis shows that the coupling strength for all interacting scenarios is quite small, and thus the models are consistent with the non-interacting w_x-cosmology. In particular, all scenarios are in agreement with $\xi = 0$

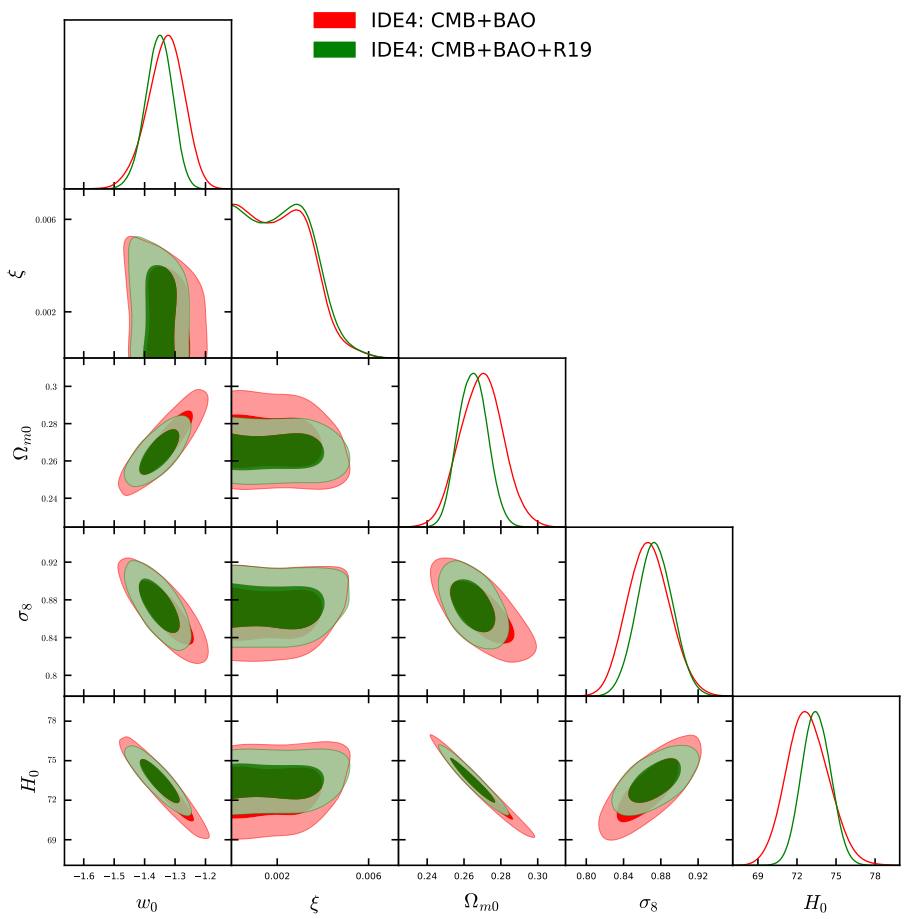


FIG. 9: *The 68% and 95% CL contour plots between various combinations of the model parameters of scenario IDE4 using only the CMB+BAO and CMB+BAO+R19 datasets, and the corresponding one-dimensional marginalized posterior distributions.*

within 2σ, but an indication for ξ greater than zero appears at 1σ when JLA and JLA+CC are added to CMB+BAO, or when R19 is added to both CMB and CMB+BAO in the IDE1 and IDE2 scenarios.

Concerning the current value of the dark energy equation of state w_0, for all interacting scenarios and for all combination of datasets it always lies in the phantom regime at more than two/three standard deviations. Moreover, we find a robust anti-correlation between w_0 and H_0.

However, the most striking feature, and one of the main results of the present work, is that for all interacting models, independently of the combination of datasets considered, the estimated values of the Hubble parameter H_0 are greater compared to the ΛCDM-based Planck's estimation [117] and close to the local measurements of H_0 from Riess et al. 2016 [118], Riess et al. 2018 [119] and Riess et al. 2019 [113]. This is triggered by the aforementioned anti-correlation between w_0 and H_0 and the strongly phantom values we obtain for w_0. The alleviation of H_0 tension is independent of the interaction model due to the absence of correlation between ξ and H_0, as shown in the two dimensional joint contours obtained for all observational datasets.

In summary, the extended interacting scenarios that include dark energy sectors with a dynamical equation of state with only one free parameter, are very efficient in alleviating the H_0 tension.

Acknowledgments

The authors thank the referee for some useful comments. SP has been supported by the Mathematical Research Impact-Centric Support Scheme (MATRICS), File No. MTR/2018/000940, given by the Science and Engineering Research Board (SERB), Govt. of India, as well as by the Faculty Research and Professional Development Fund (FRPDF) Scheme of Presidency University, Kolkata, India. WY was supported by the National Natural Science Foundation of China under Grants No. 11705079 and No. 11647153. EDV was supported from the European Research Council in the form of a Consolidator Grant with number 681431. SC acknowledges the Mathematical Research Impact Centric Sup-

Dataset	Model	$\ln B_{ij}$	Strength of evidence for reference model ΛCDM
CMB	IDE1	−2.8	Definite/Positive
CMB+BAO	IDE1	−4.6	Strong
CMB+BAO+JLA	IDE1	−7.3	Very Strong
CMB+BAO+JLA+CC	IDE1	−6.7	Very Strong
CMB+R19	IDE1	+1.0	Weak for IDE1
CMB+BAO+R19	IDE1	−0.7	Weak
CMB	IDE2	−4.3	Strong
CMB+BAO	IDE2	−4.9	Strong
CMB+BAO+JLA	IDE2	−8.3	Very Strong
CMB+BAO+JLA+CC	IDE2	−8.9	Very Strong
CMB+R19	IDE2	+1.6	Definite/Positive for IDE2
CMB+BAO+R19	IDE2	−2.2	Definite/Positive
CMB	IDE3	−2.1	Definite/Positive
CMB+BAO	IDE3	−7.6	Strong
CMB+BAO+JLA	IDE3	−8.8	Strong
CMB+BAO+JLA+CC	IDE3	−9.5	Strong
CMB+R19	IDE3	+2.0	Definite/Positive for IDE3
CMB+BAO+R19	IDE3	−1.1	Definite/Positive
CMB	IDE4	−2.0	Definite/Positive
CMB+BAO	IDE4	−5.2	Definite/Positive
CMB+BAO+JLA	IDE4	−9.6	Strong
CMB+BAO+JLA+CC	IDE4	−9.7	Strong
CMB+R19	IDE4	+0.9	Weak for IDE4
CMB+BAO+R19	IDE4	−2.3	Definite/Positive

TABLE VII: The values of $\ln B_{ij}$, where j stands for the reference model ΛCDM and i for the IDE models. The negative sign indicates that the reference model is favored over the IDE models.

port (MATRICS), File No. MTR/2017/000407, by the Science and Engineering Research Board (SERB), Government of India. This article is based upon work from CANTATA COST (European Cooperation in Science and Technology) action CA15117, EU Framework Programme Horizon 2020.

[1] E. J. Copeland, M. Sami and S. Tsujikawa, *Dynamics of dark energy,* Int. J. Mod. Phys. D **15**, 1753 (2006) [hep-th/0603057].

[2] S. Capozziello and M. De Laurentis, *Extended Theories of Gravity*, Phys. Rept. **509**, 167 (2011) [arXiv:1108.6266 [gr-qc]].

[3] Y. F. Cai, S. Capozziello, M. De Laurentis and E. N. Saridakis, *f(T) teleparallel gravity and cosmology,* Rept. Prog. Phys. **79**, no. 10, 106901 (2016) [arXiv:1511.07586 [gr-qc]].

[4] S. Nojiri, S. D. Odintsov and V. K. Oikonomou, *Modified Gravity Theories on a Nutshell: Inflation, Bounce and Late-time Evolution,* Phys. Rept. **692**, 1 (2017) [arXiv:1705.11098 [gr-qc]].

[5] C. Wetterich, *The cosmon model for an asymptotically vanishing time-dependent cosmological "constant",* Astron. Astrophys. **301**, 321 (1995) [arXiv:hep-th/9408025].

[6] L. Amendola, *Coupled Quintessence,* Phys. Rev. D **62**, 043511 (2000) [arXiv:astro-ph/9908023].

[7] L. Amendola and C. Quercellini, *Tracking and coupled dark energy as seen by WMAP,* Phys. Rev. D **68**, 023514 (2003) [arXiv:astro-ph/0303228].

[8] R. G. Cai and A. Wang, *Cosmology with interaction between phantom dark energy and dark matter and the coincidence problem,* JCAP **0503**, 002 (2005) [hep-th/0411025].

[9] D. Pavón and W. Zimdahl, *Holographic dark energy and cosmic coincidence,* Phys. Lett. B **628**, 206 (2005) [arXiv:gr-qc/0505020].

[10] S. del Campo, R. Herrera and D. Pavón, *Toward a solution of the coincidence problem,* Phys. Rev. D **78**, 021302 (2008) [arXiv:0806.2116 [astro-ph]].

[11] S. del Campo, R. Herrera and D. Pavón, *Interacting models may be key to solve the cosmic coincidence problem,* J. Cosmol. Astropart. Phys. **0901**, 020 (2009) [arXiv:0812.2210 [gr-qc]].

[12] J. D. Barrow and T. Clifton, *Cosmologies with energy exchange,* Phys. Rev. D **73**, 103520 (2006) [gr-qc/0604063].

[13] L. Amendola, G. Camargo Campos and R. Rosenfeld, *Consequences of dark matter-dark energy interaction on cosmological parameters derived from SNIa data,* Phys. Rev. D **75**, 083506 (2007) [astro-ph/0610806].

[14] J. H. He and B. Wang, *Effects of the interaction between dark energy and dark matter on cosmological parameters,* JCAP **0806**, 010 (2008) [arXiv:0801.4233 [astro-ph]].

[15] X. m. Chen, Y. g. Gong and E. N. Saridakis, *Phase-space analysis of interacting phantom cosmology,* JCAP

0904, 001 (2009) [arXiv:0812.1117 [gr-qc]].

[16] S. Basilakos and M. Plionis, *Is the Interacting Dark Matter Scenario an Alternative to Dark Energy ?,* Astron. Astrophys. **507**, 47 (2009) [arXiv:0807.4590 [astro-ph]].

[17] M. B. Gavela, D. Hernandez, L. Lopez Honorez, O. Mena and S. Rigolin, *Dark coupling,* JCAP **0907**, 034 (2009) [arXiv:0901.1611 [astro-ph.CO]].

[18] H. M. Sadjadi, $w(d) = -1$ *in interacting quintessence model,* Eur. Phys. J. C **66**, 445 (2010) [arXiv:0904.1349 [gr-qc]].

[19] M. Jamil, E. N. Saridakis and M. R. Setare, *Thermodynamics of dark energy interacting with dark matter and radiation*, Phys. Rev. D **81**, 023007 (2010) [arXiv:0910.0822 [hep-th]].

[20] X. m. Chen, Y. Gong, E. N. Saridakis and Y. Gong, *Time-dependent interacting dark energy and transient acceleration*, Int. J. Theor. Phys. **53**, 469 (2014) [arXiv:1111.6743 [astro-ph.CO]].

[21] S. Pan and S. Chakraborty, *Will there be again a transition from acceleration to deceleration in course of the dark energy evolution of the universe?,* Eur. Phys. J. C **73**, 2575 (2013) [arXiv:1303.5602 [gr-qc]].

[22] W. Yang and L. Xu, *Testing coupled dark energy with large scale structure observation,* JCAP **1408**, 034 (2014) [arXiv:1401.5177 [astro-ph.CO]].

[23] W. Yang and L. Xu, *Cosmological constraints on interacting dark energy with redshift-space distortion after Planck data,* Phys. Rev. D **89**, no.8, 083517 (2014) [arXiv:1401.1286 [astro-ph.CO]].

[24] R. C. Nunes and E. M. Barboza, *Dark matter-dark energy interaction for a time-dependent EoS parameter,* Gen. Rel. Grav. **46**, 1820 (2014) [arXiv:1404.1620 [astro-ph.CO]].

[25] V. Faraoni, J. B. Dent and E. N. Saridakis, *Covariantizing the interaction between dark energy and dark matter,* Phys. Rev. D **90**, no. 6, 063510 (2014) [arXiv:1405.7288 [gr-qc]].

[26] V. Salvatelli, N. Said, M. Bruni, A. Melchiorri and D. Wands, *Indications of a late-time interaction in the dark sector,* Phys. Rev. Lett. **113**, no. 18, 181301 (2014) [arXiv:1406.7297 [astro-ph.CO]].

[27] W. Yang and L. Xu, *Coupled dark energy with perturbed Hubble expansion rate,* Phys. Rev. D **90**, no. 8, 083532 (2014) [arXiv:1409.5533 [astro-ph.CO]].

[28] S. Pan, S. Bhattacharya and S. Chakraborty, *An analytic model for interacting dark energy and its observational constraints,* Mon. Not. Roy. Astron. Soc. **452**, no.3, 3038 (2015) [arXiv:1210.0396 [gr-qc]].

[29] Y. H. Li, J. F. Zhang and X. Zhang, *Testing models of vacuum energy interacting with cold dark matter,* Phys. Rev. D **93**, no. 2, 023002 (2016) [arXiv:1506.06349 [astro-ph.CO]].

[30] R. C. Nunes, S. Pan and E. N. Saridakis, *New constraints on interacting dark energy from cosmic chronometers*, Phys. Rev. D **94**, no. 2, 023508 (2016) [arXiv:1605.01712 [astro-ph.CO]].

[31] W. Yang, H. Li, Y. Wu and J. Lu, *Cosmological constraints on coupled dark energy,* JCAP **1610**, no.10, 007 (2016) [arXiv:1608.07039 [astro-ph.CO]].

[32] S. Kumar and R. C. Nunes, *Probing the interaction between dark matter and dark energy in the presence of massive neutrinos,* Phys. Rev. D **94**, no. 12, 123511 (2016) [arXiv:1608.02454 [astro-ph.CO]].

[33] S. Pan and G. S. Sharov, *A model with interaction of dark components and recent observational data,* Mon. Not. Roy. Astron. Soc. **472**, no. 4, 4736 (2017) [arXiv:1609.02287 [gr-qc]].

[34] A. Mukherjee and N. Banerjee, *In search of the dark matter dark energy interaction: a kinematic approach,* Class. Quant. Grav. **34**, no. 3, 035016 (2017) [arXiv:1610.04419 [astro-ph.CO]].

[35] R. Erdem, *Is it possible to obtain cosmic accelerated expansion through energy transfer between different energy densities?,* Phys. Dark Univ. **15**, 57 (2017) [arXiv:1612.04864 [gr-qc]].

[36] G. S. Sharov, S. Bhattacharya, S. Pan, R. C. Nunes and S. Chakraborty, *A new interacting two fluid model and its consequences,* Mon. Not. Roy. Astron. Soc. **466**, no. 3, 3497 (2017) [arXiv:1701.00780 [gr-qc]].

[37] M. Shahalam, S. D. Pathak, S. Li, R. Myrzakulov and A. Wang, *Dynamics of coupled phantom and tachyon fields,* Eur. Phys. J. C **77**, no. 10, 686 (2017) [arXiv:1702.04720 [gr-qc]].

[38] R. Y. Guo, Y. H. Li, J. F. Zhang and X. Zhang, *Weighing neutrinos in the scenario of vacuum energy interacting with cold dark matter: application of the parameterized post-Friedmann approach,* JCAP **1705**, no. 05, 040 (2017) [arXiv:1702.04189 [astro-ph.CO]].

[39] R. G. Cai, N. Tamanini and T. Yang, *Reconstructing the dark sector interaction with LISA,* JCAP **1705**, no. 05, 031 (2017) [arXiv:1703.07323 [astro-ph.CO]].

[40] W. Yang, N. Banerjee and S. Pan, *Constraining a dark matter and dark energy interaction scenario with a dynamical equation of state,* Phys. Rev. D **95**, no. 12, 123527 (2017) [arXiv:1705.09278 [astro-ph.CO]].

[41] L. Santos, W. Zhao, E. G. M. Ferreira and J. Quintin, *Constraining interacting dark energy with CMB and BAO future surveys,* Phys. Rev. D **96**, no. 10, 103529 (2017) [arXiv:1707.06827 [astro-ph.CO]].

[42] W. Yang, S. Pan and D. F. Mota, *Novel approach toward the large-scale stable interacting dark-energy models and their astronomical bounds,* Phys. Rev. D **96**, no. 12, 123508 (2017) [arXiv:1709.00006 [astro-ph.CO]].

[43] C. Van De Bruck and J. Mifsud, *Searching for dark matter - dark energy interactions: going beyond the conformal case,* Phys. Rev. D **97**, no. 2, 023506 (2018) [arXiv:1709.04882 [astro-ph.CO]].

[44] S. Pan, A. Mukherjee and N. Banerjee, *Astronomical bounds on a cosmological model allowing a general interaction in the dark sector,* Mon. Not. Roy. Astron. Soc. **477**, no. 1, 1189 (2018) [arXiv:1710.03725 [astro-ph.CO]].

[45] X. Xu, Y. Z. Ma and A. Weltman, *Constraining the interaction between dark sectors with future HI intensity mapping observations,* Phys. Rev. D **97**, no. 8, 083504 (2018) [arXiv:1710.03643 [astro-ph.CO]].

[46] W. Yang, S. Pan, R. Herrera and S. Chakraborty, *Large-scale (in) stability analysis of an exactly solved coupled dark-energy model,* Phys. Rev. D **98**, no. 4, 043517 (2018) [arXiv:1808.01669 [gr-qc]].

[47] W. Yang, S. Pan, L. Xu and D. F. Mota, *Effects of anisotropic stress in interacting dark matter-dark energy scenarios,* Mon. Not. Roy. Astron. Soc. **482**, no. 2, 1858 (2019) [arXiv:1804.08455 [astro-ph.CO]].

[48] W. Yang, S. Pan and A. Paliathanasis, *Cosmological constraints on an exponential interaction in the dark sector,* Mon. Not. Roy. Astron. Soc. **482**, no. 1, 1007

(2019) [arXiv:1804.08558 [gr-qc]].

[49] D. Grandon and V. H. Cardenas, *Exploring evidence of interaction between dark energy and dark matter,* Gen. Rel. Grav. **51**, no. 42 (2019) [arXiv:1804.03296 [astro-ph.CO]].

[50] S. D. Odintsov and V. K. Oikonomou, *Study of finite-time singularities of loop quantum cosmology interacting multifluids,* Phys. Rev. D **97**, no. 12, 124042 (2018) [arXiv:1806.01588 [gr-qc]].

[51] R. von Marttens, L. Casarini, D. F. Mota and W. Zimdahl, *Cosmological constraints on parametrized interacting dark energy,* Phys. Dark Univ. **23**, 100248 (2019) [arXiv:1807.11380 [astro-ph.CO]].

[52] W. Yang, N. Banerjee, A. Paliathanasis and S. Pan, *Reconstructing the dark matter and dark energy interaction scenarios from observations,* arXiv:1812.06854 [astro-ph.CO].

[53] M. Bonici and N. Maggiore, *Constraints on interacting dynamical dark energy from the cosmological equation of state,* arXiv:1812.11176 [gr-qc].

[54] M. Asghari, J. B. Jiménez, S. Khosravi and D. F. Mota, *On structure formation from a small-scales-interacting dark sector,* JCAP **1904**, no. 04, 042 (2019) [arXiv:1902.05532 [astro-ph.CO]].

[55] A. Paliathanasis, S. Pan and W. Yang, *Dynamics of nonlinear interacting dark energy models,* arXiv:1903.02370 [gr-qc].

[56] S. Pan, W. Yang, C. Singha and E. N. Saridakis, *Observational constraints on sign-changeable interaction models and alleviation of the H_0 tension,* arXiv:1903.10969 [astro-ph.CO].

[57] L. Feng, H. L. Li, J. F. Zhang and X. Zhang, *Exploring neutrino mass and mass hierarchy in interacting dark energy models,* arXiv:1903.08848 [astro-ph.CO].

[58] C. Li, X. Ren, M. Khurshudyan and Y. F. Cai, *Implications of the possible 21-cm line excess at cosmic dawn on dynamics of interacting dark energy,* arXiv:1904.02458 [astro-ph.CO].

[59] W. Yang, S. Pan, E. Di Valentino, B. Wang and A. Wang, *Forecasting Interacting Vacuum-Energy Models using Gravitational Waves,* arXiv:1904.11980 [astro-ph.CO].

[60] W. Yang, S. Vagnozzi, E. Di Valentino, R. C. Nunes, S. Pan and D. F. Mota, *Listening to the sound of dark sector interactions with gravitational wave standard sirens,* to appear in JCAP, arXiv:1905.08286 [astro-ph.CO].

[61] V. K. Oikonomou, *Generalized Logarithmic Equation of State in Classical and Loop Quantum Cosmology Dark Energy-Dark Matter Coupled Systems,* arXiv:1907.02600 [gr-qc].

[62] Y. L. Bolotin, A. Kostenko, O. A. Lemets and D. A. Yerokhin, *Cosmological Evolution With Interaction Between Dark Energy And Dark Matter,* Int. J. Mod. Phys. D **24**, no. 03, 1530007 (2015) [arXiv:1310.0085 [astro-ph.CO]].

[63] B. Wang, E. Abdalla, F. Atrio-Barandela and D. Pavón, *Dark Matter and Dark Energy Interactions: Theoretical Challenges, Cosmological Implications and Observational Signatures,* Rept. Prog. Phys. **79** (2016) no.9, 096901 [arXiv:1603.08299 [astro-ph.CO]].

[64] B. Wang, Y. g. Gong and E. Abdalla, *Transition of the dark energy equation of state in an interacting holographic dark energy model,* Phys. Lett. B **624**, 141 (2005) [hep-th/0506069].

[65] H. M. Sadjadi and M. Honardoost, *Thermodynamics second law and omega = −1 crossing(s) in interacting holographic dark energy model,* Phys. Lett. B **647**, 231 (2007) [gr-qc/0609076].

[66] S. Pan and S. Chakraborty, *A cosmographic analysis of holographic dark energy models,* Int. J. Mod. Phys. D **23**, no. 11, 1450092 (2014) [arXiv:1410.8281 [gr-qc]].

[67] E. Di Valentino, A. Melchiorri and J. Silk, *Beyond six parameters: extending ΛCDM,* Phys. Rev. D **92**, no. 12, 121302 (2015) [arXiv:1507.06646 [astro-ph.CO]].

[68] E. Di Valentino, A. Melchiorri and J. Silk, *Reconciling Planck with the local value of H_0 in extended parameter space,* Phys. Lett. B **761**, 242 (2016) [arXiv:1606.00634 [astro-ph.CO]].

[69] S. Kumar and R. C. Nunes, *Echo of interactions in the dark sector,* Phys. Rev. D **96**, no. 10, 103511 (2017) [arXiv:1702.02143 [astro-ph.CO]].

[70] E. Di Valentino, A. Melchiorri and O. Mena, *Can interacting dark energy solve the H_0 tension?,* Phys. Rev. D **96**, no. 4, 043503 (2017) [arXiv:1704.08342 [astro-ph.CO]].

[71] E. Di Valentino, A. Melchiorri, E. V. Linder and J. Silk, *Constraining Dark Energy Dynamics in Extended Parameter Space,* Phys. Rev. D **96**, no. 2, 023523 (2017) [arXiv:1704.00762 [astro-ph.CO]].

[72] J. Renk, M. Zumalacárregui, F. Montanari and A. Barreira, *Galileon gravity in light of ISW, CMB, BAO and H_0 data,* JCAP **1710**, no. 10, 020 (2017) [arXiv:1707.02263 [astro-ph.CO]].

[73] E. Di Valentino, *Crack in the cosmological paradigm,* Nat. Astron. **1**, no. 9, 569 (2017) [arXiv:1709.04046 [physics.pop-ph]].

[74] E. Di Valentino, C. Bøehm, E. Hivon and F. R. Bouchet, *Reducing the H_0 and σ_8 tensions with Dark Matter-neutrino interactions,* Phys. Rev. D **97**, no. 4, 043513 (2018) [arXiv:1710.02559 [astro-ph.CO]].

[75] D. Fernandez Arenas *et al.*, *An independent determination of the local Hubble constant*, Mon. Not. Roy. Astron. Soc. **474**, no. 1, 1250 (2018) [arXiv:1710.05951 [astro-ph.CO]].

[76] E. Di Valentino, E. V. Linder and A. Melchiorri, *Vacuum phase transition solves the H_0 tension,* Phys. Rev. D **97**, no. 4, 043528 (2018) [arXiv:1710.02153 [astro-ph.CO]].

[77] N. Khosravi, S. Baghram, N. Afshordi and N. Altamirano, *H_0 tension as a hint for a transition in gravitational theory,* Phys. Rev. D **99**, no. 10, 103526 (2019) [arXiv:1710.09366 [astro-ph.CO]].

[78] E. Mörtsell and S. Dhawan, *Does the Hubble constant tension call for new physics?,* JCAP **1809**, no. 09, 025 (2018) [arXiv:1801.07260 [astro-ph.CO]].

[79] W. Yang, S. Pan, E. Di Valentino, R. C. Nunes, S. Vagnozzi and D. F. Mota, *Tale of stable interacting dark energy, observational signatures, and the H_0 tension,* JCAP **1809**, no. 09, 019 (2018) [arXiv:1805.08252 [astro-ph.CO]].

[80] F. D'Eramo, R. Z. Ferreira, A. Notari and J. L. Bernal, *Hot Axions and the H_0 tension,* JCAP **1811**, no. 11, 014 (2018) [arXiv:1808.07430 [hep-ph]].

[81] W. Yang, A. Mukherjee, E. Di Valentino and S. Pan, *Interacting dark energy with time varying equation of state and the H_0 tension,* Phys. Rev. D **98**, no. 12, 123527 (2018) [arXiv:1809.06883 [astro-ph.CO]].

[82] R. Y. Guo, J. F. Zhang and X. Zhang, *Can the H_0 tension be resolved in extensions to ΛCDM cosmology?,* JCAP **1902**, 054 (2019) [arXiv:1809.02340 [astro-ph.CO]].

[83] W. Yang, S. Pan, E. Di Valentino, E. N. Saridakis and S. Chakraborty, *Observational constraints on one-parameter dynamical dark-energy parametrizations and the H_0 tension,* Phys. Rev. D **99** no.4, 043543 (2019), arXiv:1810.05141 [astro-ph.CO].

[84] V. Poulin, T. L. Smith, T. Karwal and M. Kamionkowski, *Early Dark Energy Can Resolve The Hubble Tension,* Phys. Rev. Lett. **122**, no. 22, 221301 (2019) [arXiv:1811.04083 [astro-ph.CO]].

[85] X. Zhang and Q. G. Huang, *Constraints on H_0 from WMAP and baryon acoustic osillation measurements,* arXiv:1812.01877 [astro-ph.CO].

[86] C. D. Kreisch, F. Y. Cyr-Racine and O. Doré, *The Neutrino Puzzle: Anomalies, Interactions, and Cosmological Tensions,* arXiv:1902.00534 [astro-ph.CO].

[87] M. Martinelli, N. B. Hogg, S. Peirone, M. Bruni and D. Wands, *Constraints on the interacting vacuum - geodesic CDM scenario,* arXiv:1902.10694 [astro-ph.CO].

[88] K. L. Pandey, T. Karwal and S. Das, *Alleviating the H_0 and σ_8 anomalies with a decaying dark matter model,* arXiv:1902.10636 [astro-ph.CO].

[89] K. Vattis, S. M. Koushiappas and A. Loeb, *Dark matter decaying in the late Universe can relieve the H0 tension,* Phys. Rev. D **99**, no. 12, 121302 (2019) [arXiv:1903.06220 [astro-ph.CO]].

[90] S. Kumar, R. C. Nunes and S. K. Yadav, *Dark sector interaction: a remedy of the tensions between CMB and LSS data,* Eur. Phys. J. C **79**, no. 7, 576 (2019) [arXiv:1903.04865 [astro-ph.CO]].

[91] P. Agrawal, F. Y. Cyr-Racine, D. Pinner and L. Randall, *Rock 'n' Roll Solutions to the Hubble Tension,* arXiv:1904.01016 [astro-ph.CO].

[92] W. Yang, S. Pan, E. Di Valentino, A. Paliathanasis and J. Lu, *Challenging bulk viscous unified scenarios with cosmological observations,* arXiv:1906.04162 [astro-ph.CO].

[93] W. Yang, O. Mena, S. Pan and E. Di Valentino, *Dark sectors with dynamical coupling,* arXiv:1906.11697 [astro-ph.CO].

[94] E. Di Valentino, R. Z. Ferreira, L. Visinelli and U. Danielsson, *Late time transitions in the quintessence field and the H_0 tension,* arXiv:1906.11255 [astro-ph.CO].

[95] W. Yang, S. Pan, S. Vagnozzi, E. Di Valentino, D. F. Mota and S. Capozziello, *Dawn of the dark: unified dark sectors and the EDGES Cosmic Dawn 21-cm signal,* arXiv:1907.05344 [astro-ph.CO].

[96] A. Pourtsidou and T. Tram, *Reconciling CMB and structure growth measurements with dark energy interactions,* Phys. Rev. D **94**, no. 4, 043518 (2016) [arXiv:1604.04222 [astro-ph.CO]].

[97] R. An, C. Feng and B. Wang, *Relieving the Tension between Weak Lensing and Cosmic Microwave Background with Interacting Dark Matter and Dark Energy Models,* JCAP **1802**, no. 02, 038 (2018) [arXiv:1711.06799 [astro-ph.CO]].

[98] E. Di Valentino and S. Bridle, *Exploring the Tension between Current Cosmic Microwave Background and Cosmic Shear Data,* Symmetry **10**, no. 11, 585 (2018).

[99] W. Yang, S. Pan and J. D. Barrow, *Large-scale Stability and Astronomical Constraints for Coupled Dark-Energy Models,* Phys. Rev. D **97**, no. 4, 043529 (2018) [arXiv:1706.04953 [astro-ph.CO]].

[100] V. F. Mukhanov, H. A. Feldman and R. H. Brandenberger, *Theory of cosmological perturbations,* Phys. Rept. **215**, 203 (1992).

[101] C. P. Ma and E. Bertschinger, *Cosmological perturbation theory in the synchronous and conformal Newtonian gauges,* Astrophys. J. **455**, 7 (1995) arXiv:astro-ph/9506072.

[102] K. A. Malik and D. Wands, *Cosmological perturbations,* Phys. Rept. **475**, 1 (2009) [arXiv:0809.4944 [astro-ph]].

[103] E. Majerotto, J. Valiviita and R. Maartens, *Adiabatic initial conditions for perturbations in interacting dark energy models,* Mon. Not. Roy. Astron. Soc. **402**, 2344 (2010) [arXiv:0907.4981 [astro-ph.CO]].

[104] J. Väliviita, E. Majerotto and R. Maartens, *Instability in interacting dark energy and dark matter fluids,* JCAP **0807**, 020 (2008) [arXiv:0804.0232 [astro-ph]].

[105] T. Clemson, K. Koyama, G. B. Zhao, R. Maartens and J. Valiviita, *Interacting Dark Energy – constraints and degeneracies,* Phys. Rev. D **85**, 043007 (2012) [arXiv:1109.6234 [astro-ph.CO]].

[106] R. Adam *et al.* [Planck Collaboration], *Planck 2015 results. I. Overview of products and scientific results,* Astron. Astrophys. **594**, A1 (2016) [arXiv:1502.01582 [astro-ph.CO]].

[107] N. Aghanim *et al.* [Planck Collaboration], *Planck 2015 results. XI. CMB power spectra, likelihoods, and robustness of parameters,* Astron. Astrophys. **594**, A11 (2016) [arXiv:1507.02704 [astro-ph.CO]].

[108] M. Betoule *et al.* [SDSS Collaboration], *Improved cosmological constraints from a joint analysis of the SDSS-II and SNLS supernova samples,* Astron. Astrophys. **568**, A22 (2014) [arXiv:1401.4064 [astro-ph.CO]].

[109] F. Beutler *et al.*, *The 6dF Galaxy Survey: Baryon Acoustic Oscillations and the Local Hubble Constant,* Mon. Not. Roy. Astron. Soc. **416**, 3017 (2011) [arXiv:1106.3366 [astro-ph.CO]].

[110] A. J. Ross, L. Samushia, C. Howlett, W. J. Percival, A. Burden and M. Manera, *The clustering of the SDSS DR7 main Galaxy sample I. A 4 per cent distance measure at $z = 0.15$,* Mon. Not. Roy. Astron. Soc. **449**, no. 1, 835 (2015) [arXiv:1409.3242 [astro-ph.CO]].

[111] H. Gil-Marín *et al.*, *The clustering of galaxies in the SDSS-III Baryon Oscillation Spectroscopic Survey: BAO measurement from the LOS-dependent power spectrum of DR12 BOSS galaxies,* Mon. Not. Roy. Astron. Soc. **460**, no. 4, 4210 (2016) [arXiv:1509.06373 [astro-ph.CO]].

[112] M. Moresco *et al.*, *A 6% measurement of the Hubble parameter at $z \sim 0.45$: direct evidence of the epoch of cosmic re-acceleration,* JCAP **1605**, no. 05, 014 (2016) [arXiv:1601.01701 [astro-ph.CO]].

[113] A. G. Riess, S. Casertano, W. Yuan, L. M. Macri and D. Scolnic, *Large Magellanic Cloud Cepheid Standards Provide a 1% Foundation for the Determination of the Hubble Constant and Stronger Evidence for Physics Beyond LambdaCDM,* arXiv:1903.07603 [astro-ph.CO].

[114] A. Lewis and S. Bridle, *Cosmological parameters from CMB and other data: A Monte Carlo approach,* Phys. Rev. D **66**, 103511 (2002) [astro-ph/0205436].

[115] A. Lewis, A. Challinor and A. Lasenby, *Efficient com-*

putation of CMB anisotropies in closed FRW models, Astrophys. J. **538**, 473 (2000) [astro-ph/9911177].

[116] N. Aghanim *et al.* [Planck Collaboration], *Planck 2018 results. VI. Cosmological parameters,* [arXiv:1807.06209 [astro-ph.CO]].

[117] P. A. R. Ade *et al.* [Planck Collaboration], *Planck 2015 results. XIII. Cosmological parameters,* Astron. Astrophys. **594**, A13 (2016) [arXiv:1502.01589 [astro-ph.CO]].

[118] A. G. Riess *et al.*, *A 2.4% Determination of the Local Value of the Hubble Constant,* Astrophys. J. **826**, no. 1, 56 (2016) [arXiv:1604.01424 [astro-ph.CO]].

[119] A. G. Riess *et al.*, *New Parallaxes of Galactic Cepheids from Spatially Scanning the Hubble Space Telescope: Implications for the Hubble Constant*, Astrophys. J. **855**, 136 (2018).

[120] A. Heavens, Y. Fantaye, A. Mootoovaloo, H. Eggers, Z. Hosenie, S. Kroon and E. Sellentin, *Marginal Likelihoods from Monte Carlo Markov Chains,* arXiv:1704.03472 [stat.CO].

[121] A. Heavens, Y. Fantaye, E. Sellentin, H. Eggers, Z. Hosenie, S. Kroon and A. Mootoovaloo, *No evidence for extensions to the standard cosmological model,* Phys. Rev. Lett. **119**, no. 10, 101301 (2017) [arXiv:1704.03467 [astro-ph.CO]].

[122] R. E. Kass and A. E. Raftery, *Bayes Factors,* J. Am. Statist. Assoc. **90**, no.430, 773 (1995).